Motors for use in molecular nanotechnology

Klok, Martin

Chapter 6
Design, synthesis and characterisation of a molecular walker system

In this chapter the design principles of a molecular system, that in principle should be capable of linear translational motion upon irradiation, is outlined. The design is based on a rigid scaffold combining two molecular rotor subunits, that connect to traditional stator parts via parallel axles, with the stators oriented in opposite direction. Such a design gives rise to a molecule that features two rotating wheels, which, depending on the diastereomeric identity, rotate in equal or opposite directions. Principles of design are discussed, and synthetic approaches featuring naphthalene, dibenzo[1,4]dioxin and benzo[c]chromene scaffolds have been investigated. The benzo[c]chromene approach leads to two molecular double motors that are characterised by a variety of spectroscopic methods. Photochemical experiments confirm that the motor function is preserved, and widefield single molecule spectroscopy allows for tracking of translational motion on glass and mica surfaces. STM-images of these structures correlate with single molecules being observed.

6.1 Introduction

Crossing the barrier from interesting science to the development of potentially applicable devices requires the field of molecular nanotechnology to gain control of motion at the molecular level. This can be considered the Holy Grail of the field, and as such the subject is given much thought.[1] Four dimensions over which control of motion can be achieved theoretically are being distinguished, being time (rate of motion), and the 3 basic coordinates x, y and z. The lowest level of control is then control over time, a form of control in which we can influence the rate, but not the direction of motion of molecules. In other words, the lowest level of control over molecular motion is the control over diffusion, and several attempts in this direction have been made.[2] An attempt to use overcrowded alkene-based molecular motor systems to achieve this failed for reasons that are understandable in retrospect, which has been described in chapter 4.

A higher level of theoretically achievable control over molecular motion is to control not only the rate, but also the direction of motion. The simplest example of this is a molecule that moves in a straight line. Nature has provided us with ample examples of its feasibility.[3] By motion along an existing 1-dimensional trail x, the other 2 degrees of freedom y and z are effectively discarded, resulting in controlled molecular motion along a straight line.

A much greater challenge is to gain control over two degrees of freedom for molecular motion. In that case, motion can be controlled not only in the x-direction, but 'steered' in x- and y-directions. This can only be achieved on a surface or some other form of interface, where the two directions are predefined. Finally, full control over molecular motion is achieved in three coordinates (x, y, z) in time, which should be the final theoretical goal. However, due to the random forces associated with Brownian motion, as yet no evident approaches to perform this exist; even nature's abundant array of examples does not provide us with clues of how to achieve this.

A way to partly disable Brownian motion to a large extent is to adsorb a potentially moving structure to a surface. If the Van der Waals forces that facilitate the absorption are strong enough, the structure will remain in place without drifting, despite the heavy motion of solvent (or air) molecules just above and onto the adsorbed structure. A large central structure, possibly with characteristics favouring experimental detection, is therefore anticipated to provide a chance of achieving this. In such case, repetitive unidirectional motion of wheels attached to the side of the scaffold could allow for one-dimensional controlled linear motion when the wheels are rotating in the same direction. Synthetically this may be challenging as during

synthesis it is likely that a mixture of diastereomers is obtained. In this case, the meso compound will have the wheels rotating in the same direction, whereas the *RR* and *SS* enantiomers will have the wheels rotating in opposite directions (Figure 1).

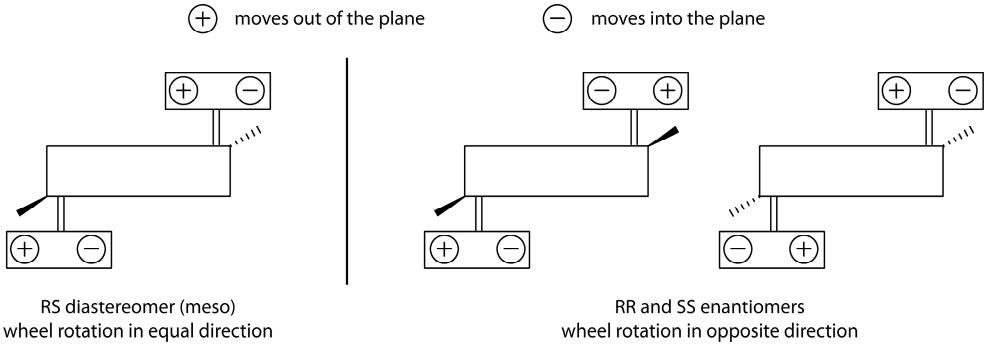

Figure 1: Direction of wheel rotation for diasteromeric possibilities of a molecular walker.

In the case of the meso compound, two mechanisms to provide linear motion can be distinguished (Figure 2). First of all, mechanism 1 can be considered, in which the wheels rotate one by one by *cis* – *trans* isomerisation and subsequent thermal helix inversion. This mechanism relies on the assumption that rotation of the wheel, with the scaffold bound reversibly to the surface, creates some form of friction, resulting in a forward force. Which wheel undergoes isomerisation is not predefined, as excitation of the full structure could result in double bond isomerisation of both the front and the back axle. Which one isomerises is effectively a chance-based process, and for the case of equal stators the probability is around 0.5 for both stators. However, with the axles parallel and the wheels on different sides of the scaffold, a series of rotations would result in an average forward motion. Whether the friction that is required actually exists cannot be estimated from research data at this point; however, mechanical considerations are is support of this assumption given that the surface interactions are just right. Apart from that, the existence of rolling molecular motion can be considered indicative of the presence of a form of friction at this level.[4] Any directional reorientation by Brownian motion would disturb the linearity of the line of motion, so it is evident that the full structure in absence of wheel rotation should be as motionless as possible. If that is so, even a low rate of rotation would result in controllable translational motion. On these grounds, some form of linear translational motion is anticipated if mechanism 1 is found to be valid.

Elaborating on this mechanism, steering of the structure in two dimensions is then on the horizon. By adapting the structure to have two separate wheels featuring a different quantum yield of *cis* – *trans* isomerisation, a curved trajectory would be

expected, based on what axle has a higher probability of isomerisation, and the orientation on the surface. In this case, the chance of isomerisation would be different for one axle relative to the other. The curvature of motion is the result of a small sideward force associated with rotation of an axle oriented sideward of the scaffold, by the sideward component of the force resultant from the friction required in this mechanism. Another possibility that should be investigated is wavelength-directed steering: by preferential excitation of either the front or the back part of the molecule by different absorption characteristics of the stators it may be possible to influence which side undergoes isomerisation, creating controlled bents by the same sideward force component of the rotating wheel. For this approach to work, the excited state of the molecule should not be homogeneous, but rather excitation of one part of the molecule should result in a higher chance of that axle isomerising. The molecule should thus consist of more or less separated photochemical 'subunits', which is a well-proven possibility. For instance, the possibility of intramolecular energy transfer is indicative of the possibility of having separate photochemically active parts in the same molecule.[5] However, energy transfer in itself presents a complication in such systems, as these processes are hard to predict or control.

A second mechanism can be envisioned as well (mechanism 2 in Figure 2). Double bond isomerisation could lead to rotation of the scaffold with respect to the

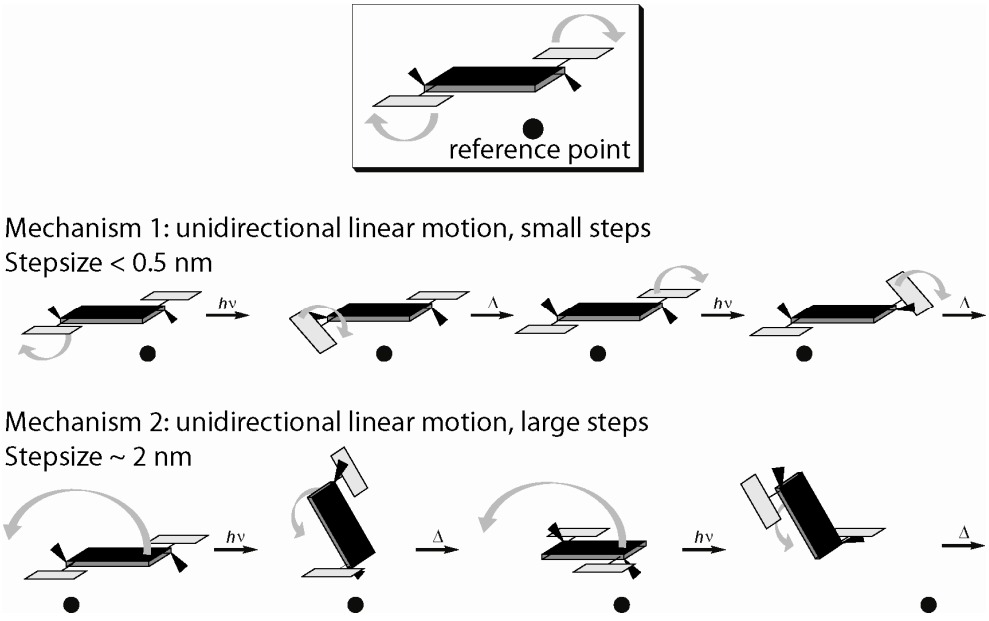

Figure 2: Schematic picture of possible mechanisms for molecular walking.

stator, in which case the stator would remain on the surface. If the frictional forces of rotation of the stator with respect to the surface in a small volume are larger than the forces associated with motion of the scaffold through a large volume, this mechanism is expected to be favoured. Especially in the case of experiments on solid surfaces in the absence of solvent (*i.e.* surface – air or surface – vacuum interfaces) this might well be the case, because of the large free volume available in such conditions. Several advantages of this mechanism over the previous mechanism can be distinguished: first of all, the step size becomes larger, as the scaffold in most cases would be larger than the stator. Secondly, the randomness of which double bond isomerises will be removed; a preference for isomerisation of the front axle will be present, as the back axle cannot rotate in this mechanism. Assuming absence of directional reorientation by Brownian motion, a highly linear pathway is expected due to alternate isomerisation of both axels. However, the probability of directional reorientation by Brownian motion is higher in this case than for mechanism 1, as most of the structure becomes detached from the surface for a relatively long time. An average detachment time of about one half-life time for thermal helix inversion is expected.

From this line of reasoning a general design for a molecular walker system that is capable of moving in a straight line in one direction was constructed (Figure 2). In general terms, we envision a rigid scaffold, which connects two unidirectionally rotating substructures functioning as legs or wheels. With two units that do ½ rotations alternately on average, this structure would follow a more or less linear path as described above. Chiral methylcyclopentylidene units connected to standard stators make up the unidirectional 'wheels', and the rigidity of the middle piece ensures a proper spatial arrangement of rotating subunits. At the same time, the aromaticity and size of the scaffold presents the possibility of fluorescent properties, allowing for widefield fluorescence spectroscopy and STM as viable experimental detection tools. However, the success of such a project relies on the synthesis of a structure that has its wheels rotating in the same absolute direction.

6.2 Naphthalene-based molecular walkers

6.2.1 Retrosynthesis

The first step to achieve controlled molecular movement is the realisation of linear movement, to be achieved by a molecular double-motor. Staying as close as possible to the original motor structure, structures **1** and **2** were identified as a potential synthetic goal. A retrosynthetic analysis is presented in Scheme 1. Attachment of two, rather than one methylcyclopentylidene units to a central naphthalene unit would turn the naphthalene unit into the envisioned central scaffold **3**. Coupling to two stator units in a double Barton-Kellogg reaction then results in a

structure compliant with the definition above. A major advantage of this approach is that the structure remains as close to the original motor molecule as possible, so that physical properties are expected to be preserved. On the other hand, the double functionalisation required for this approach is unfavourable. Especially the Barton-Kellogg reaction, which is challenging even under favourable conditions, is expected to result in low yields when attempting it on two sites of the same molecule at the same time.

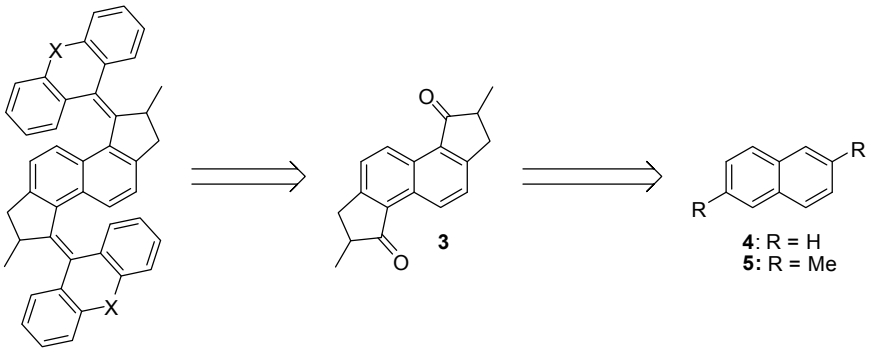

Scheme 1: Retrosynthetic analysis of double motors **1** and **2**.

6.2.2 Synthesis

In analogy to well-established methods for obtaining cyclopentylidene rotors,[6] direct naphthalene functionalisation according to Scheme 2 was attempted, but failed to result in the formation of bisketone **3**. For this reason, a different route was devised starting from 2,6-dimethylnaphthalene **5** (Scheme 3). Because commercially available **5** consists of 5% regioisomers, this compound was prepared pure according to a literature procedure.[7] Bromination of the methyl groups using NBS and irradiation in benzene solution afforded bisbromide **6** in 70% yield. In an adaptation of a literature procedure,[8] **6** was reacted with the sodium salt of methyl diethyl malonate to provide the bismalonate derivative **7** in 92% yield. This product was not isolated, but

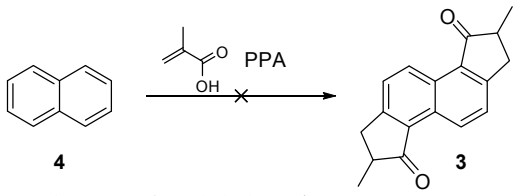

Scheme 2: Direct functionalisation of naphthalene **4**.

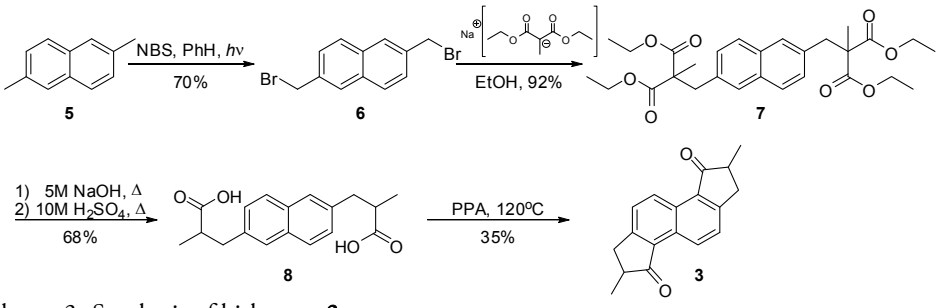

Scheme 3**:** Synthesis of bisketone **3.**

transformed directly into the free acid using NaOH solution, and subsequently decarboxylated in H_2SO_4 to give the methylpropionic acid derivative **8** in 70% yield. This compound was cyclised in PPA at 120 ºC to give bisketone **3** in 53% yield (33% from dibromide **6**).

A double Barton-Kellogg procedure was envisioned for the coupling reaction, which turned out to be complicated. As neither bisthione **10** nor bishydrazone **11** is

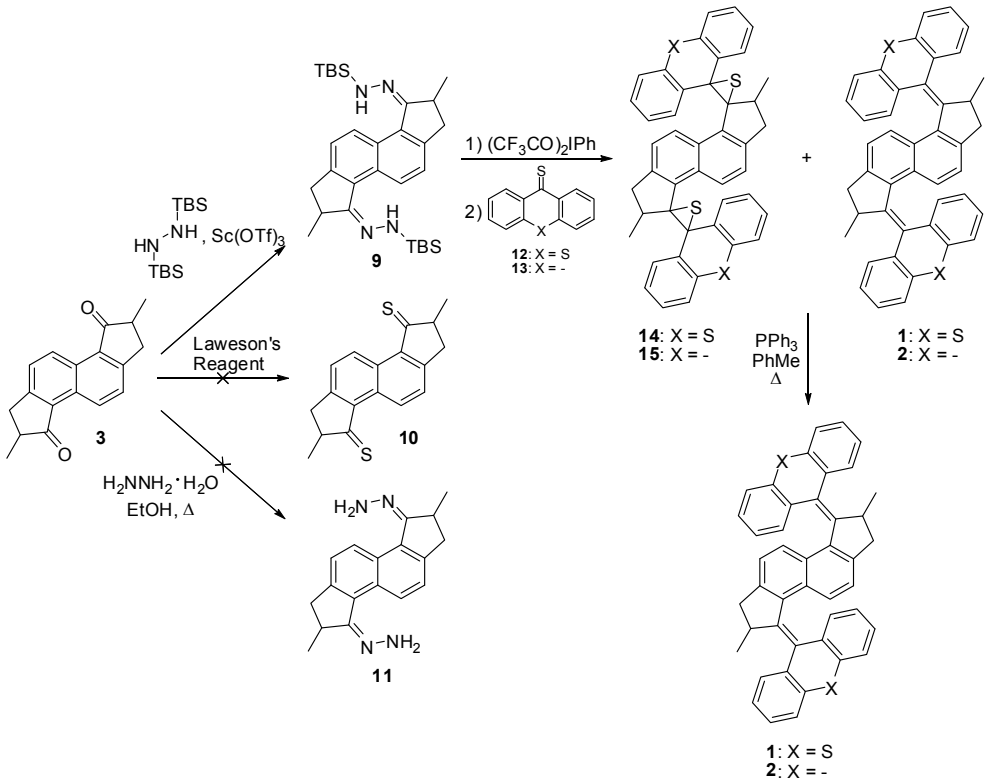

Scheme 4: Coupling of bisketone **3** with stator parts **12** and **13**.

stable, we were required to proceed via the TBDMS-protected hydrazone **9** (Scheme 4). This could be prepared by reaction in pure TBDMS-protected hydrazine (3 eq.) in the presence of 5% $Sc(OTf)_3$ at 100 °C.[9] As it was found that deprotection occurred *in situ* under the conditions for coupling, pure TBDMS-hydrazone **9** was reacted with freshly prepared 9*H*-fluorene-9-thione **13** to provide a small (<<10%) quantity of episulfide **15**, which was desulphurised using PPh_3 in toluene to result in an essentially insoluble compound, which could not be characterised. Alternatively, reaction of **9** with 9*H*-thioxanthene-9-thione **12** resulted in a mixture of episulfides and alkenes, that was desulphurised using PPh_3 to give a highly insoluble compound that by mass spectroscopy and ^{1}H NMR spectroscopy could be identified as bismotor **1**. However, the insolubility of the compound(s) precluded purification of the crude product(s), so that well-defined experiments on the photochemical behaviour were out of reach.

Preliminary photochemical experiments on the crude product mixture **1** did not provide reproducible results, such as a distinct change in the UV/Vis-spectrum upon irradiation, under circumstances where the parent motor (**7** in chapter 2) gave clear conversion to the higher energy isomer. Furthermore, fluorescence spectroscopy revealed that this compound displayed at most very weak emission. Because of the difficulties associated with the synthetic route, solubility and purification, this approach to obtain a structure according to Figure 2 was not pursued further.

6.3 Bisbenzo[1,4]dioxin-based molecular walkers

6.3.1 Retrosynthesis

To increase solubility and enhance the fluorescence quantum yield, a second synthetic target was indentified as having two molecular motor moieties centered onto

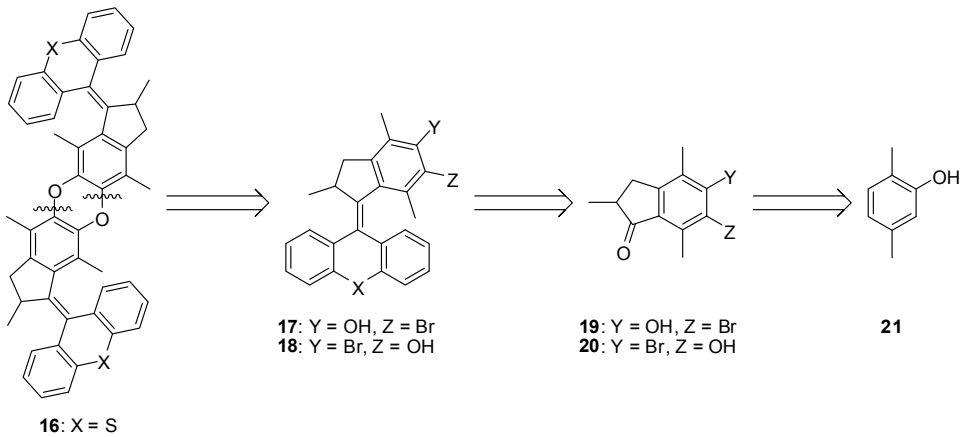

16: X = S

17: Y = OH, Z = Br
18: Y = Br, Z = OH

19: Y = OH, Z = Br
20: Y = Br, Z = OH

21

Scheme 5: Retrosynthesis of dibenzo[1,4]dioxin-based motor **16**.

a dibenzo[1,4]dioxin scaffold. A retrosynthesic approach is shown in Scheme 5. A symmetric dissection of the dioxin bonds in **16** results in free phenolic motors **17** and **18** as convenient material for dibenzo[1,4]dioxin coupling.

Although a motor structure featuring a xylene rotor and a thioxanthone stator such as **17** or **18** has not been prepared before, molecular modelling indicates that the expectation of motor behaviour is quite reasonable for such compounds. The rotor part of **16** has been described before, and was found to result in a small increase in the rate of thermal helix inversion when connected to a fluorenylidene stator, in comparison to naphthalene analogues.[6] As the stator part of **16** has been shown to result in high rates of thermal helix inversion when connected to a cyclopentylidene rotor (chapter 2), molecular double motor **16** is expected to display rates of thermal helix inversion higher than its naphthalene analogue (presented in chapter 2 as compound **7**). This means that the anticipated rate of thermal helix inversion lies above 6.5×10^{6} s^{-1} at 20 °C. According to the discussion in chapter 2, high energy differences between the stable and unstable form(s) in combination with an inherent helical shape of the molecule in all of its conformations should result in unidirectional motor behaviour, also in cases where experimental verification of the thermal pathways is difficult to realise. In the absence of better methods, and in view of the synthetic accessibility and functionalisability of such rotor structures, DFT-verification of the isomeric possibilities of the base motor (Y = Z = H for **17** and **18**, see Figure 3) seems worthwhile. The inherent uncertainty associated with this approach is recognised, but we expect some predictive value because the experiments in chapter 3 display good correlation between experimental and calculated data. Since the predicted rates of the processes associated with motor function lie at timescales that are difficult to access experimentally (chapter 2), calculated data on this structure are considered a valuable extension to the research into molecular double motor **16**.

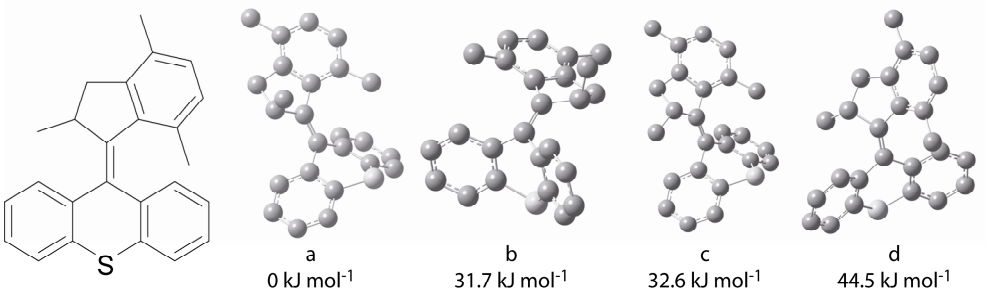

Figure 3: Conformations and relative energies of the single motor that makes up molecular double motor **16**.

Analysis of the minima along the reaction coordinate for isomerisation of the central double bond using DFT calculation (B3LYP, 6-31G(d,p)) indicates similar geometries as found for the compounds described in chapter 3. The lowest energy conformation was found to be *anti*-folded, with the methyl substituent oriented in an axial orientation (a in Figure 3). A second local minimum with the methyl substituent oriented in a pseudo-equatorial orientation and an anti-folded overall conformation is comparable with minima found in chapter 3 (c in Figure 3). Furthermore, a *syn*-folded conformation with the methyl substituent oriented in an axial orientation is present (b in Figure 3). Similar to the naphthalene analogue in chapter 3, the xylene rotor in this case results in a highly twisted minimum on the reaction coordinate, with the methyl substituent oriented in equatorial orientation (d in Figure 3). Conformations b, c and d have higher energy by 31.7, 32.6 and 44.5 kJ mol^{-1}, respectively. The transition state between c and b is calculated to have an energy 47.1 kJ mol^{-1}, and is the same as the transition state for conversion of c to a. Data on the immediate photochemical product have not been obtained and should be subject of further research, as is experimental verification of the reaction pathway. However, these data indicate that the steric hindrance in this structure is sufficient to result in large energy differences between the stable and unstable forms, rendering the thermal equilibrium quantitatively on the side of the most stable isomer and effecting unidirectional helix inversion. As photochemical *cis – trans* isomerisation is expected to occur for the central double bonds of **16** just as it does for all other stilbene-like double bonds, there is no reason to assume other than unidirectional behaviour for this compound. For this reason, we anticipate unidirectional rotation for structure **16**.

Based on these results, and the results obtained for structure **8** in chapter 2 it is therefore assumed that **16** will display a rate of thermal helix inversion above 6.5×10^{6} s^{-1} at 20 °C. For this reason, these xylene-functionalised molecular motors will be assumed to display unidirectional behaviour with high rates for thermal helix inversion upon irradiation.

An advantage of the synthetic approach in Scheme 5 is the high degree of convergence and the associated easy adaptation of the route to coupling different stator units onto the same scaffold. Apart from that, the symmetric bond cleavage allows for only a single regioisomer (2 diastereomers among which 1 pair of enantiomers) as the theoretical outcome of the coupling reaction. Disadvantages are the dioxin coupling, which is not a well-known reaction for electron-rich dibenzodioxins (*vide infra*), and the requirement of a free motor phenol, which for cyclopentylidene rotors has not been isolated before.

It has been shown that deprotection of a methoxy group on a cyclopentylidene rotor results in degradation of the structure.[10] Similar attempts using a TBDMS protecting group resulted in highly unstable though isolable products for a first generation molecular motor,[10a] but reproduction of this reaction proved tedious. For this reason, another protecting group with mild deprotecting conditions that would survive the coupling reaction was required. Methoxymethyl (MOM) protection was chosen as a suitable candidate. Provided that acid is not used during workup, the MOM-group will remain intact; the smallest amounts of acid will initiate its removal.

A special feature in this approach is that the identity of the indanone is not predefined: both 6-bromo-5-hydroxy-2,4,7-trimethylindan-1-one **19** and 5-bromo-6-hydroxy-2,4,7-trimethylindan-1-one **20** would couple to yield the same product **16**. However, the fact that these compounds are electronically different may prove useful in the final dioxin coupling procedure. Although **19** is expected to be favoured during formation of the ketone, **20** should not be discarded.

6.3.2 Benzo[1,4]dioxin coupling

Benzodioxins are a highly toxic class of chemicals, notorious for long biotic lifetimes and environmental impact, especially the chlorinated and brominated derivatives.[11] Although traditionally only minor interest in the preparation of these compounds exists due to their high toxicity, more recently an interest into the preparation of substituted dibenzo[1,4]dioxins has grown, driven by the discovery of potential biomedical properties.[12]

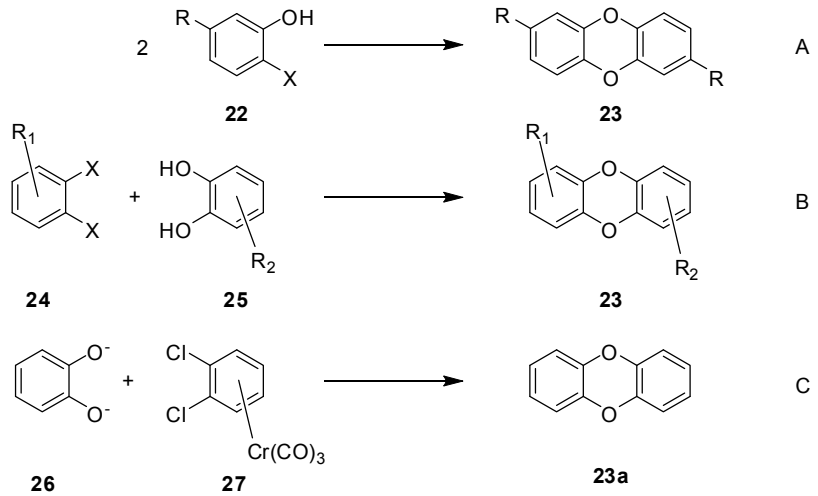

Scheme 6: Methods for the preparation of bisbenzo[1,4]dioxins.

According to a paper by Lee and Denny,[13] three main routes toward these compounds are known (Scheme 6): condensation of *o*-halophenols in the presence of base gives products **23**, albeit in low yields (10 – 20%, method A). The reaction has been used to prepare the symmetric compound (R = H),[14] as well as functionalised analogues.[15] It is not fully regiospecific as one would expect,[16] which is attributed to the occurrence of a Smiles rearrangement during synthesis (Scheme 7).[17] However, it is not clear whether this is general for all reaction conditions, and the ratio of products formed appears to be product-driven, so that the regiospecificity might be controlled by steric or electronic factors. Two different halophenols have also been used, which resulted in a complex though separable product mixture.[18]

More convenient is the coupling between catechol and activated *o*-chlorobenzenes (method B in Scheme 6). Although it is not regiospecific, this reaction has been used to prepare asymmetrically substituted products in 10 – 25% yield.[19] In these reactions, nitro activation is often used to promote chloro substitution, although the absence of nitro-substituted products indicates that it also acts as a preferential leaving group.[19b] Nitro-activation is not necessary however, as it is found that polychlorobenzenes are suitable candidates in this reaction as well.[20]

More recently, other halogens have been used in this method; cyano- and nitro activated fluoro displacement has been described by Eastmond and Swanson to

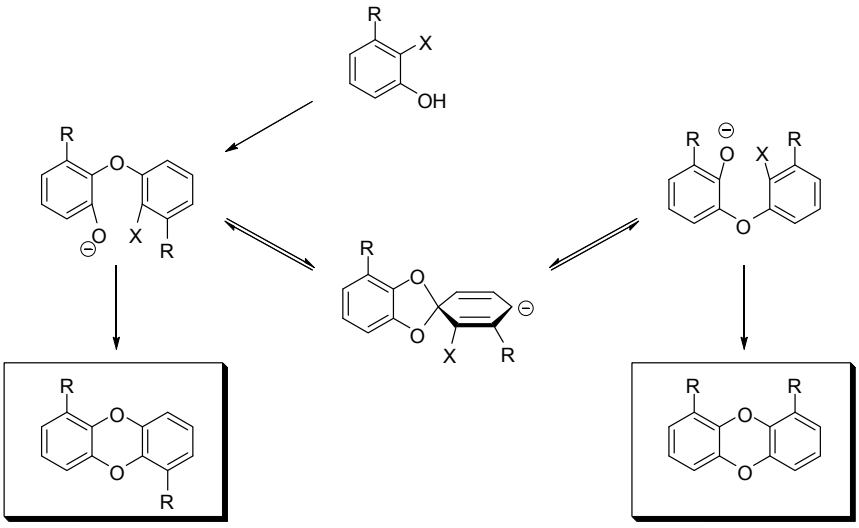

Scheme 7: Smiles rearrangement (adapted from ref. 18).

proceed in high yield (90 – 100%),[21] diiodobenzenes can be coupled to 2,3-dihydroxynaphthalene in 2 – 25 % yield[22] and dibromobenzenes and difluorobenzenes can be coupled with 2,3-dihydroxynaphthalene,[23] with activated fluorobenzenes giving the better yields. Interestingly, the reaction conditions tested in this work were also tested on related halophenols according to route A, but failed to provide any product.

Alternatively, halogen activation has been achieved using organometallic reagents (method C): tricarbonylchromium[24] as well as cyclopentadienyliron[25] complexes have been reported to result in dibenzo[1,4]dioxin in reasonable to high yield, but the formation of the complex itself cannot be achieved efficiently, which renders this method not attractive synthetically.

However, the methods described generally suffer from low yields, and all require harsh conditions. High temperatures, alkali metals or copper (salts) and/or strong bases are required for the formation of **23**, and also in cases where only a single regioisomer would be expected (method A), a mixture of regioisomeric products is sometimes obtained.

As the synthetic path to obtain isomerically pure **16** is much shorter using *o*-halophenols, method A is the pathway of choice despite the general literature preference for method B. In addition, as motor molecules generally are much less stable than the compounds described for these couplings, harsh conditions for the coupling will have to be avoided.

For this reason, a method for well-defined benzo[1,4]dioxin-coupling using *o*-halosubstituted phenols will have to be developed. Numerous procedures for the preparation of diphenyl ethers are known,[26] and aryl-O bond formation is covered by an even a larger scope of possibilities, among which copper[27] and palladium[28] couplings are the most prominent. As among these approaches relatively mild methods prevail, it is possible that a method can be identified that yields dibenzo[1,4]dioxin **16** according to Scheme 8. Regiochemistry might be driven by the steric bulk of the reactant, suppressing, partly at least, the Smiles rearrangement that would result in complex product mixtures. As moieties **17** and **18** are difficult to access, tests for this reaction were performed using 2-bromo-3,6-dimethylphenol **28**[29] using various reaction conditions.

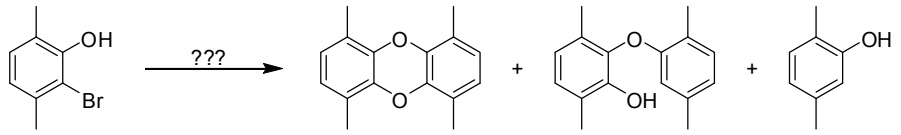

28 **29** **30** **21**

Scheme 8: Symmetric dibenzo[1,4]dioxin coupling via *o*-bromophenol **28**, with common side products.

In a first attempt, palladium-based couplings were tried using literature procedures for the formation of diaryl ethers.[30] However, the use of 2-(di-*tert*-butylphosphino)biphenyl **31**, 2-dicyclohexylphosphino-2'-4'-6'-triisopropylbiphenyl, (XPhos, **32**) or the more hindered analogue 2-di-*tert*-butylphosphino-2'-4'-6'-triisopropylbiphenyl (di-*t*BuXphos, **33**, Figure 4) provided only minor amounts of **29**, the main product being **21**. The conditions used (1.0 eq. **28**, 2.0 eq. K_3PO_4, 2% $Pd(OAc)_2$ and 3% ligand in 0.3 M dry toluene at 100 °C, 24 h) represent optimised conditions for the formation of electron-rich, sterically hindered biaryl ethers, for which application of **33** results in 92% yield of 2,5-dimethyl-*o*-xylyl ether. The absence of required product **29**, or partly coupled but reduced product **30** validates no further work in the direction of palladium-assisted couplings.

In an attempt to use copper as the catalyst, a first attempt was made using Ullmann conditions (DMF and Cu(s) in the presence of 1 eq of K_2CO_3 at reflux). Although these conditions are estimated to be far from suitable for the formation of final product **16**, the resulting product mixture of **29** and **30** with only a minor amount of **21** gave some confidence for finding suitable copper-mediated conditions.

As several studies noted that the use of additives and different copper sources favour milder reaction conditions,[31] an initial screening was performed to identify a method toward **29**. As can be seen from Table 1, **29** was formed in most cases, but side products **30** and **21** were formed as well. Molecular sieves (4 Å) were found to have no effect on the reaction, but the addition of ca 10% TMHD to a NMP solution was found to suppress the formation of side products. However, these conditions did

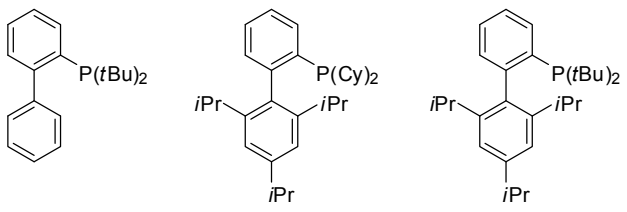

31 **32** **33**

Figure 4: Ligands used in the palladium-assisted coupling of **28**.

not result in formation of **29** in more than 20% yield. More success was obtained using the CuBr-SMe_2 complex in acetonitrile; 41% product yield was obtained under these conditions.[32] For this reason, it was estimated that after a systematic optimisation, the reaction of **28** to **29** should be possible in reasonable yield using relatively mild reaction conditions. However, free phenol **17** or **18** is required, and at this point it was not certain whether such compounds could be obtained.

Reagent	Solvent	Base	additive	T [°C]	products
Cu	DMF	x	x	50-130	**21, 29,30**
CuI	DMF	$CsCO_3$	x	120	**21, 30**
$Cu(PPh_3)Br$	DMF	$CsCO_3$	x	100 - 130	**29, 30**
$Cu(PPh_3)Br$	NMP	$CsCO_3$	Molsieves	70	**21, 29, 30**
$Cu(PPh_3)Br$	NMP	$CsCO_3$	Molsieves TMHD*	100-130	**29** (20%)
$Cu(PPh_3)Br$	PhMe	$CsCO_3$	x	110	**21**
Cu_2O	Pyr	x	x	115	**21**
CuBr-SMe_2	MeCN	$CsCO_3$	pyridine	70	**29** (41%)

* TMHD = tetramethylheptanedione

Table 1: Conditions for reaction of **28** to yield **29** based on literature procedures for the formation aryl ethers.[31]

6.3.3 Bisbenzo[1,4]dioxin molecular walker synthesis

Two possible routes are envisioned to obtain ketones **19** and **20**: preparation of bromide **28** and subsequent cyclisation to obtain **19** and/or **20**, or alternatively preparation of indanones **34** and/or **35**, and subsequent bromination (Scheme 9). In the first case, bromination of 2,5-dimethylphenol **21** according to a literature procedure[29] gave bromophenol **28**. Several procedures, among which reaction of methacrylic acid in PPA and Friedel-Crafts reaction with α-methyl-β-chloropropionic acid chloride to obtain the indanone from this compound were attempted, but neither free phenol **28** nor its methyl- or TBS protected analogues provided **19** or **20** (Scheme 10). In contrast, reaction of methyl-protected xylene **36** gave a good yield of the desired indanones **37** and **38** as a mixture of isomers, which could be separated by column chromatography. Deprotection of the methyl ether and subsequent bromination did not result in the desired compounds **19** and **20**, instead dibromo compounds **39** and **40** were obtained by a combination of aromatic- and α-bromination. As removal of an α-bromine has been reported as a facile procedure,[33] and because the bromination of **34** and **35** occurred readily, this procedure proved satisfying to obtain the product indanones. Before coupling to stator parts though, the

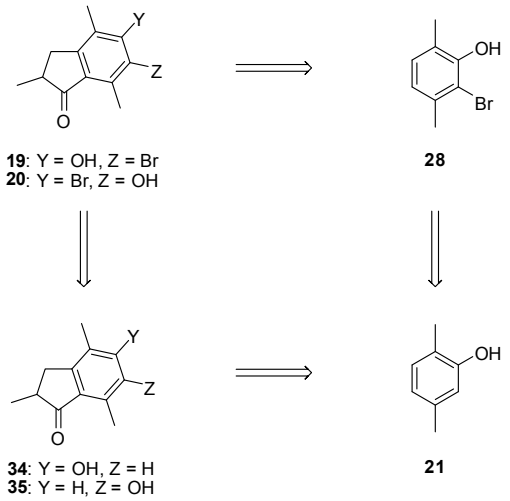

Scheme 9: Two possible pathways to ketones **19** and **20**.

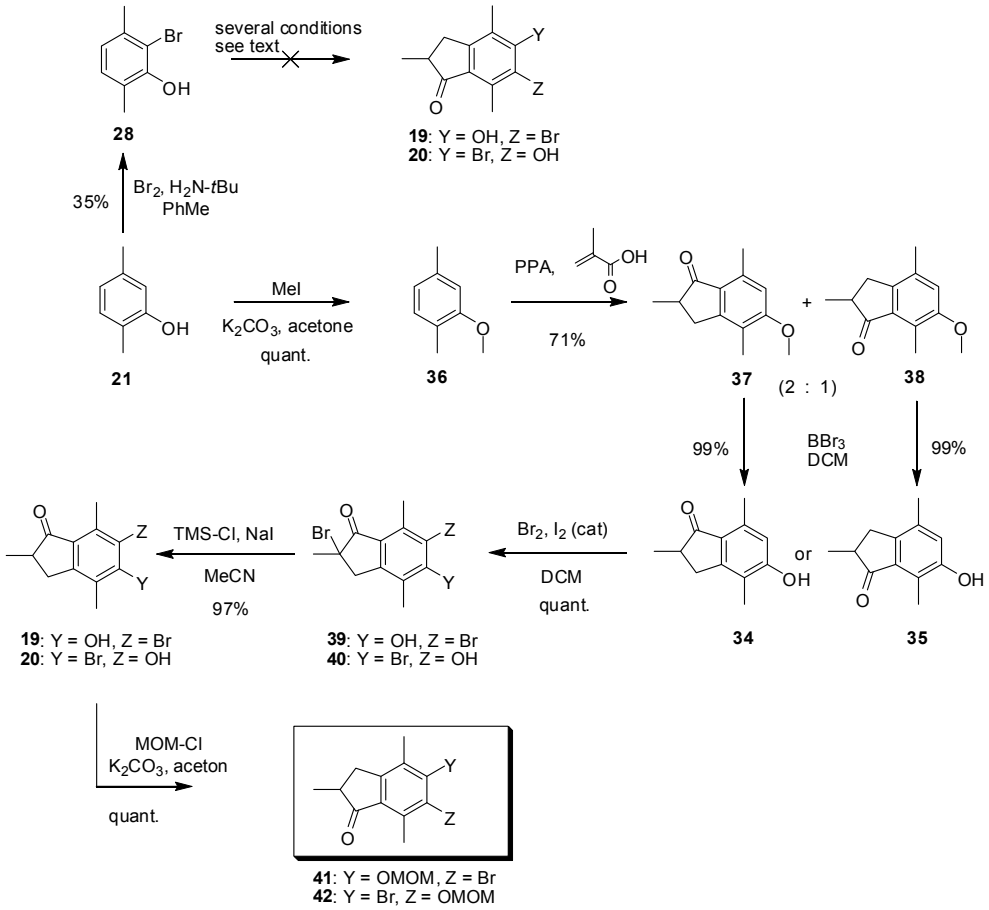

Scheme 10: Synthesis of the rotor part of benzo[1,4]dioxin based molecular double motors.

choice was made to protect the phenol, to minimise the chances of failure in the Barton Kellogg coupling. The methoxymethyl (MOM) group was chosen because of the very mild conditions necessary for its removal (**41** and **42**, Scheme 10).

6.3.4 Barton-Kellogg coupling

The Barton-Kellogg reaction has proven the only attractive option so far for the preparation of 2nd generation motors, and therefore is the method of choice for the

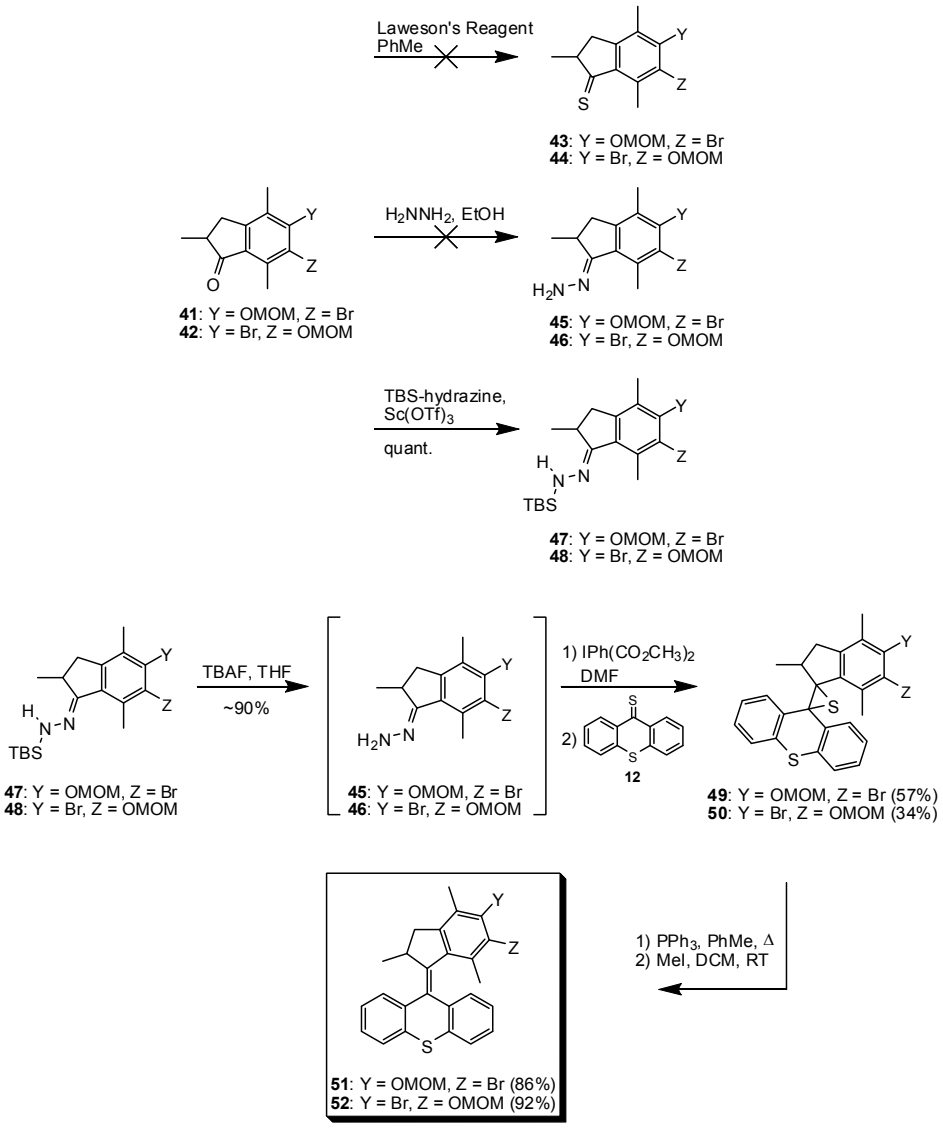

Scheme 11: The Barton-Kellogg coupling of **41** and **42** to thioxanthone thioketone **12**.

preparation of **16**. However, indanones **41** and **42** could not be converted to their respective hydrazones or thioketones (Scheme 11). Attempts to obtain pure thioketone resulted in messy thiol mixtures, rather than thiones **43** or **44**. Reaction with hydrazine hydrate resulted in degradation, and small quantities of isolated material were debrominated, for which reason this approach was not pursued further. Reaction with TBS-protected hydrazine as described above however did result in the pure TBS-protected hydrazones **47** and **48**. Deprotection using TBS-Cl gave the hydrazones **45** and **46** in approximately 90% yield. These compounds turned out to be unstable and had to be used in the coupling directly, which explains the degradation products found by direct reaction with hydrazine hydrate.

Oxidation of **45** or **46** using diacetoxyiodobenzene and subsequent reaction with 9*H*-thioxanthene-9-thione **12** in DMF/DCM resulted in episulfides **49** and **50**. Subsequent reaction with triphenyl phosphine resulted in motor compounds **51** and **52**, which were isolated after a total of 10 steps in 20% and 6% yield, respectively.

Deprotection of the MOM-group of motor compounds **51** and **52** proved to be challenging. HCl in DCM resulted in double bond shift of the central double bond, as indicated by ^{1}H NMR spectroscopy. Variation of the procedure gave indications that isomerisation was the result of the presence of water and acid or base during reaction and/or workup. Therefore, the reaction was performed using dry DCM and TFA under N_2, followed by the addition of EtOAc. Rapid addition of H_2O followed by a very small amount of saturated bicarbonate and immediate separation of the layers provided compound **53** with 95% purity, the other 5% being the isomeric compound **54** (Scheme 12). Compound **53** can be crystallised from Et_2O with ease from the product mixture, and is stable as a solid or in dry solution.

In contrast, motor compound **52** could be deprotected without observable isomerisation by the same procedure (Scheme 13). An explanation for this difference in reactivity can be found in the following mechanism (Scheme 14). With the hydroxyl group of **53** in conjugation to the double bond, acid and base can form the isomeric cyclohexadienone **56**, which is driven to the isomerised product **54** by the lower energy of this compound relative to **53** by a formal 1,3-H-shift. Motor **55** does not have a favourable resonance structure involving the hydroxyl group and the central double bond, which is why this compound is easier to deprotect (Scheme 14).

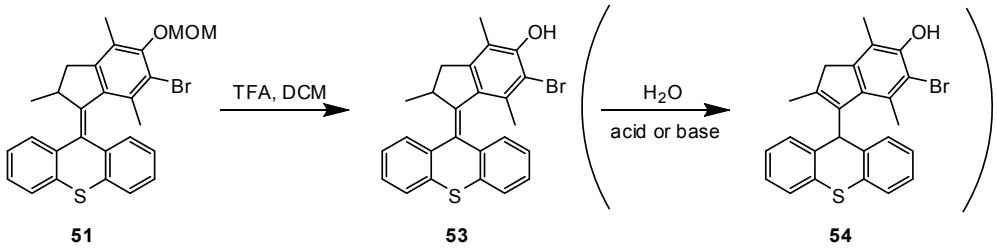

51 **53** **54**

Scheme 12: Deprotection of motor compound **51**.

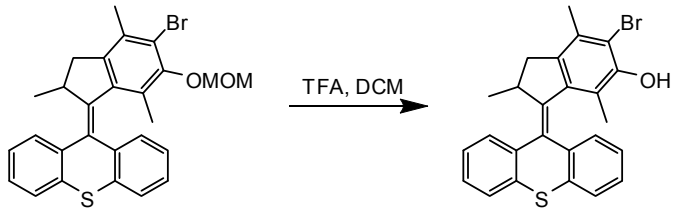

52 **55**

Scheme 13**:** Deprotection of motor compound **52.**

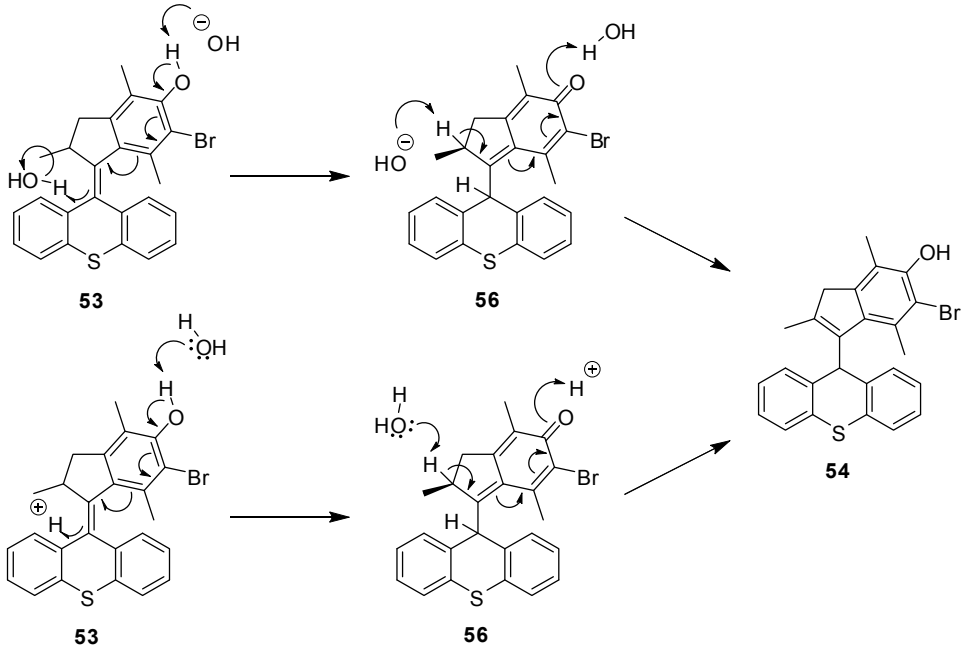

Scheme 14: Isomerisation by double bond shift through acid or base catalysis.

6.3.5 Dibenzo[1,4]dioxin coupling of molecular motors

In the final step, coupling of two molecules **53** or two molecules **55** was envisioned. In the case of **53**, using a $CuBr{\cdot}SMe_2$ complex in the presence of $CsCO_3$ and pyridine in refluxing acetonitrile under dry-nitrogen conditions, the coupling resulted in a mixture of products, from which only a low yield of the coupled product **57** could be identified by mass spectrometry and ^1H NMR spectroscopy. Double bond shift was complete for this compound, as was observed by the appearance of similar singlets for the single double bond shifted product **54** and the disappearance of diastereotopic cyclopentylidene ring protons. Apart from that, similar to double bond-shifted product **54**, the protons of the xanthone stator did not appear in their characteristic pattern, but instead were reduced to two multiplets, a strong indication of the presence of a single bond between former stator and rotor.

Deprotection of the other isomer was easier, resulting in **55** as the starting point for dibenzo[1,4] dioxin coupling. Using the same conditions as described above resulted in double motor **16** as a mixture of isomers (Scheme 16). The presence of these compounds was verified by ^1H NMR and mass spectroscopy; important arguments for identification are the cyclopentylidene ring protons and associated the methyl doublet, as well as the strong difference in shift between the aromatic methyl peaks. Moreover, the stator aromatic protons display the same 6-fold pattern as observed for **52**. However, apart from the anticipated *RR*/SS and *RS* isomers, the number of signals indicated the presence of more isomers. Therefore it is assumed that steric factors do not direct the reaction to the desired product **16** exclusively, but instead regioisomers are obtained. As the central scaffold is not stable on common column chromatography supports, purification of these materials is tedious, and was not successful.

An explanation for the results on the coupling reactions can be sought in the Smiles rearrangement (Scheme 7), in combination with the envisioned mechanism for double bond shift (Scheme 14). In case of compound **53**, it is found that even in dry

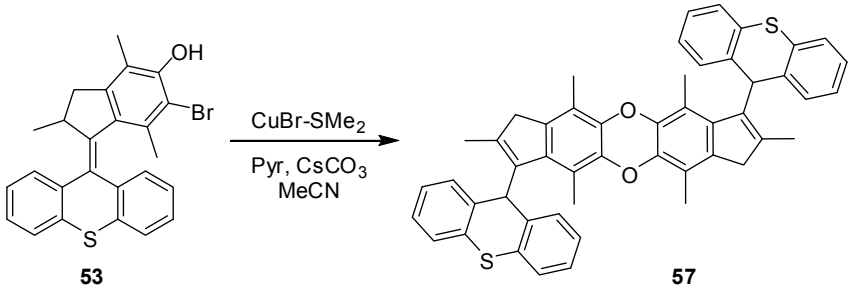

53 **57**

Scheme 15: Final coupling of **53**, resulting in the double bond-shifted dibenzo[1,4]dioxin **57**.

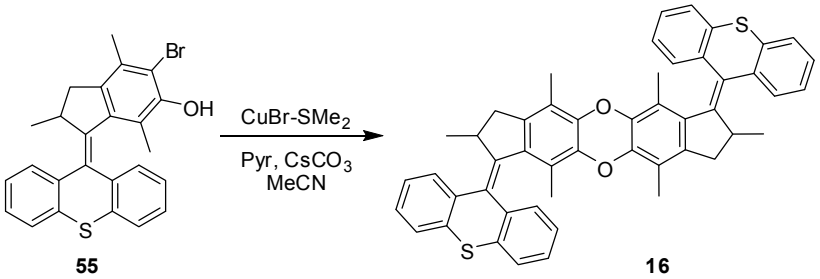

Scheme 16: Final coupling of **55**, resulting in the double motor functionalised dibenzo[1,4]dioxin **16** as a mixture of regioisomers.

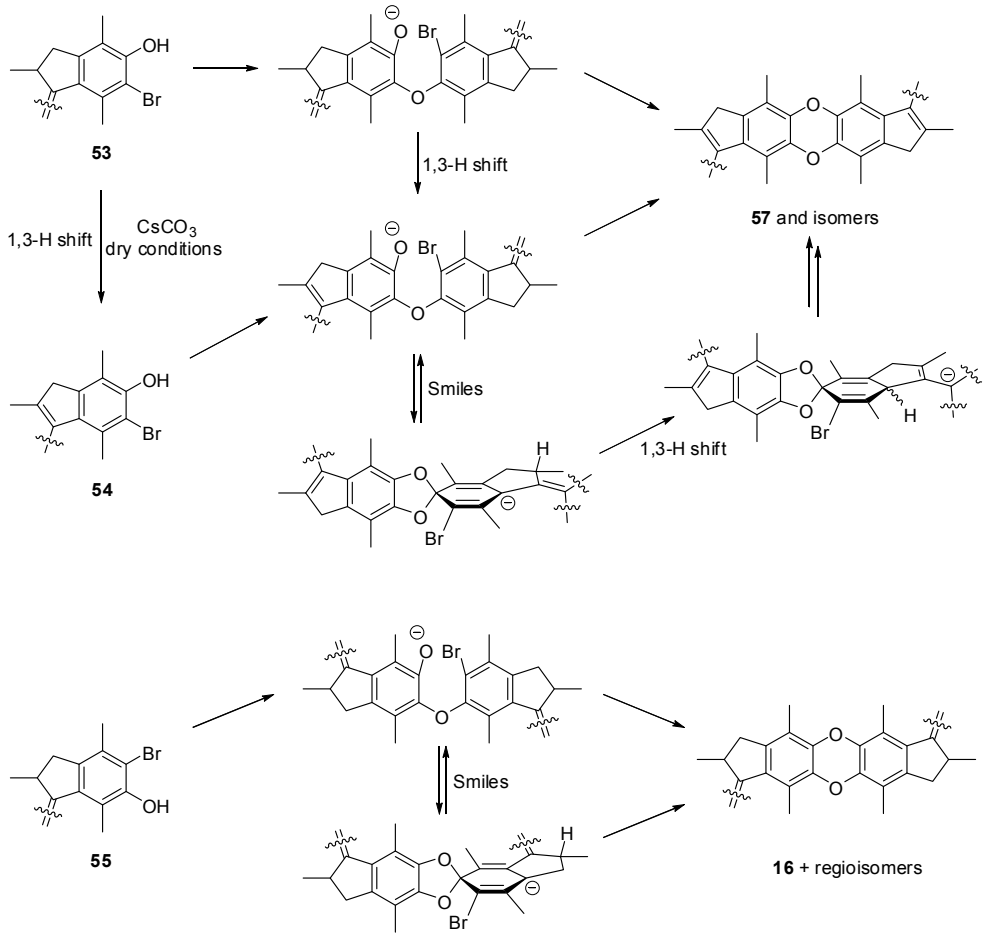

Scheme 17: Dibenzo[1,4]dioxin coupling for compounds **53** and **55**.

conditions, a 1,3-hydrogen shift can occur; working under anhydrous conditions does not suppress it, as was the case in the synthesis of **53**. The presence of base alone is sufficient for a fast 1,3-hydrogen shift to occur. The coupling reaction seems to occur however, albeit slower than the double bond shift (Scheme 17). In case of **55**, the lack of conjugation suppresses the double bond shift, and in this case **16** is obtained, as a mixture of regioisomers due to Smiles rearrangement. It is found that steric repulsion of stator moieties does not drive the reaction exclusively to the less hindered product, as was initially hoped for.

6.3.6 Dibenzo[1,4]dioxin photochemistry

With the publication of the mechanism of photodegradation of dibenzo[1,4]dioxins this project required a revision.[34] Upon irradiation with 300 nm light, in a variety of organic and aqueous solutions, dibenzo[1,4]dioxin and a variety of 2,3,6,7-tetrasubstituted analogues resulted in the corresponding dihydroxybiphenyl as the major photoproduct, and varying amounts of hydroxydibenzofuran and 2-phenoxyphenol as minor products. Some polymeric material remained uncharacterised. Polar protic solvents are found to be markedly more efficient in this reaction, whereas in apolar aprotic solvents such as toluene or hexane conversion to the dihydroxybiphenyl is much lower. Triplet quenching studies show that the photodegradation process goes via the singlet state for both conversions. The mechanism of formation was reported to proceed via transient 2,2'-biphenylquinones, which form dihydroxybiphenyls photochemically. In the absence of steady-state irradiation and the in the presence of electron donating groups, a thermal pathway to the oxepino[2,3-b]benzofuran is accessible, whereas the presence of electron withdrawing groups results thermally in hydroxybenzofurans (Scheme 18). A pH effect was not observed, and the main factor for determining the photoproduct was found to be solvent polarity.

With the pathway of photochemical degradation of the scaffold known, little hope exists that dibenzo[1,4]dioxin-based molecular double motor **16** will display sufficient photochemistry for repetitive photochemical – thermal cycles as required for prolonged motor-like functioning. Continuous irradiation would presumably result in the oxepino[2,3-b]benzofuran **61**, as kinetic isotope effects for proton transfer from solvent to the excited bisquinone **59** indicate that this process is not possible in common organic solvents such as benzene or toluene.[34] The presence of small amounts of water or other proton sources during irradiation would, however, result in different isomers of the dihydroxybiphenyls **60**. For this reason, attempts to vary / optimise the preparative procedure were not undertaken, and photochemical experiments were not performed.

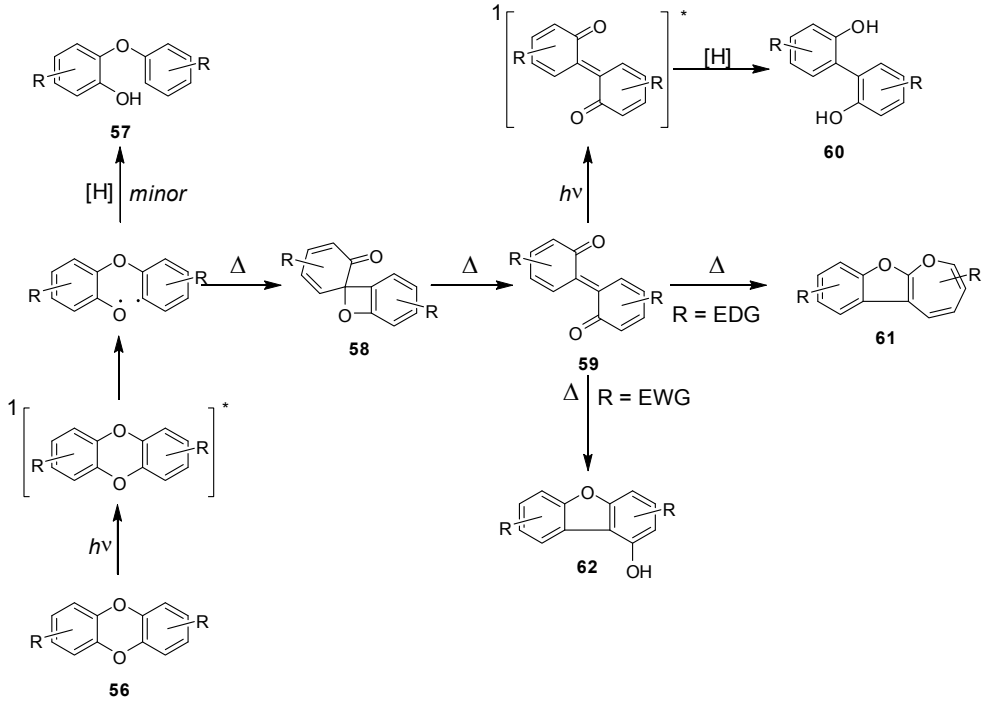

Scheme 18: Mechanism for photodegradation of dibenzo[1,4]dioxin 56 (Reproduced from ref 34).

6.4 6*H*-benzo[c]chromene-based molecular walkers

A viable synthetic approach toward a rigid scaffold functionalised with molecular motors can be represented by the terphenyl structure given in Figure 5. Despite its apparent complexity, this structure is relatively straightforward to prepare. Various approaches for obtaining a molecular double motor according to Figure 2 can be considered, and as possible photochemical activity of the scaffold is not expected to result in degradation or isomerisation, this structure is perceived as a viable basis for a functioning molecular double motor.

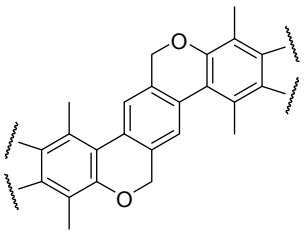

Figure 5: Bis(benzo[c]chromene) scaffold for preparation of a molecular double motor.

Data on the photochemical stability of this scaffold can be obtained by careful study of the mechanism of two photochemical reactions. Photochemical studies on xanthene **63** indicate that the final product from irradiation is 6*H*-benzo[c]chromene **68** (Scheme 19).[35] Although experiments in highly polar solvents, such as H_2O-MeCN or MeOH, indicate that photochemical interconversion as depicted in Scheme 19 as **66** – **69** interconversion is possible, photolysis of chromene **68** resulted in only a very small conversion to the (hydroxyphenyl)benzyl alcohol **69**. The mechanism for this reaction is known, and involves a similar quinone intermediate, **66**, as observed for dibenzo[1,4]dioxin photodegradation. However, these studies have only been performed in the highly polar media H_2O-MeCN and MeOH, as addition of water is required for conversion to the (hydroxyphenyl)benzyl alcohol **69**. Other nucleophiles than water allow for different pathways, as exemplified by the conversion to **67** in the presence of MeOH. It is assumed that in case the quinone **66** results from irradiation of chromene **68**, it has no other option but to revert to the original structure as long as water is absent. When some water is present, **69** might result, but this is converted photochemically to **66**, which reverts thermally to **68**. Based on the concerted nature of formation of the chromene **68** it is likely that biphenyl isomerisation does not take

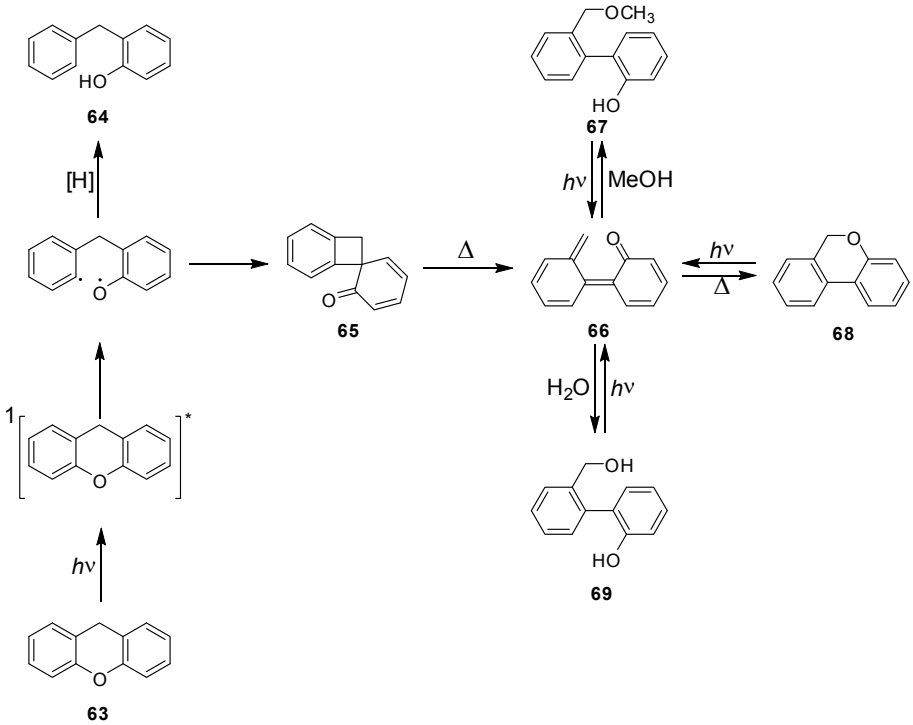

Scheme 19: Photochemical pathway from xanthene **63** to chromene **68**, and possible photochemical conversions of chromene **68** (adapted from ref 36).

place during this process. Racemisation of the terphenyl substructure does not affect the expected functioning of a molecular double motor constructed on this scaffold, especially as it is likely that racemisation by restricted rotation around the biphenyl bond in chromene **68** is possible thermally at room temperature. Therefore, if apart from photochemical *cis - trans* isomerisation a second photochemical reaction pathway via quinone **66** were possible for a double motor based on this scaffold, it is expected that this extra photochemical equilibrium does not result in abundant degradation or isomerisation of the double motor. Only temporal deactivation might occur, restoring the original molecular walker scaffold **68** either photochemically (**69** → **66**) or thermally (**66** → **68**). Aromatic methyl substitution in **70** and **71** will prevent formation of the isomeric form **69**, minimising photochemical side reactions.

6.4.1 Retrosynthesis

The retrosynthesis for molecular double motors based on a bis(6*H*-benzo[c]chromene) scaffold can be seen in Scheme 20. Although all steps look feasible on paper, a drawback of this approach is the linearity, and the associated double-sided

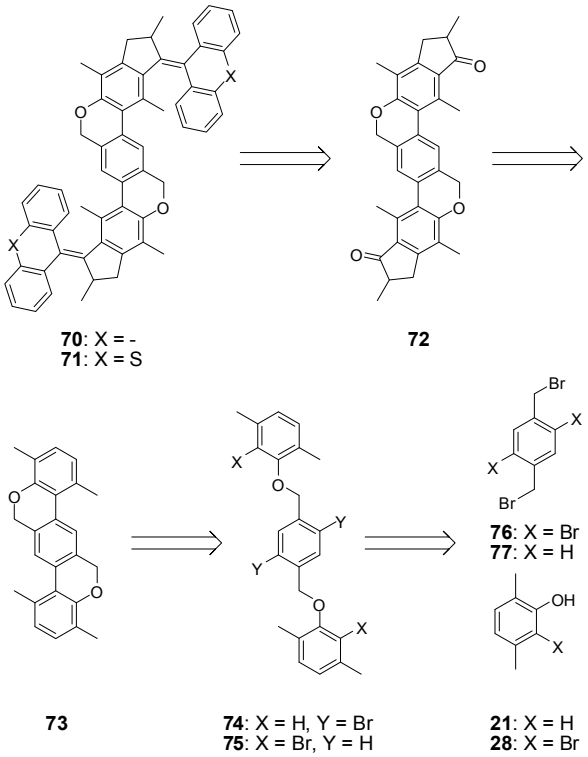

Scheme 20: Retrosynthesis of a molecular double motor based on a bis(benzo[c]chromene) scaffold.

reactivity in much of the steps, which will decrease yields. Especially double formation of the indanone **72**, and the double Barton-Kellogg reaction are expected to be challenging to perform with sufficient yield.

6.4.2 Synthesis

Compound **76** was prepared following a literature procedure.[36] Reaction of **21** with **76** in the presence of K_2CO_3 in acetone afforded the highly insoluble compounds **74** and **75.** The reaction of **28** was much slower under the same reaction conditions as used for reaction of **21**, even when heating the reaction mixture. Purification of **74** and **75** from mono-coupled product and starting material was straightforward due to the low solubility.

Compound **74** could be cyclised using a literature procedure for biphenyl formation[37] in quantitative yield. The same reaction with compound **75** resulted in varying quantities of di-cyclised product, the remainder being monocyclised and debrominated side products (Scheme 21).

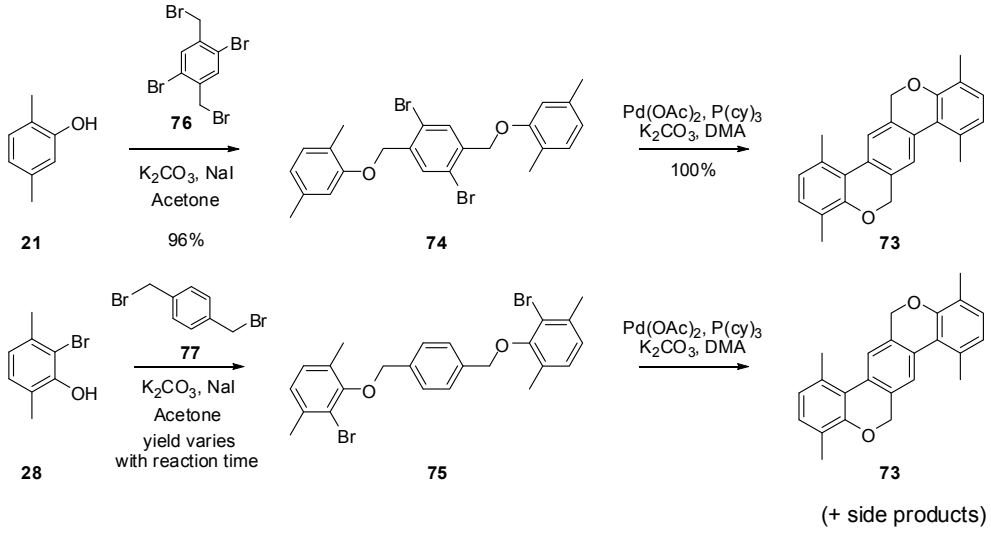

Scheme 21: Preparation of the bis(benzo[c]chromene) scaffold.

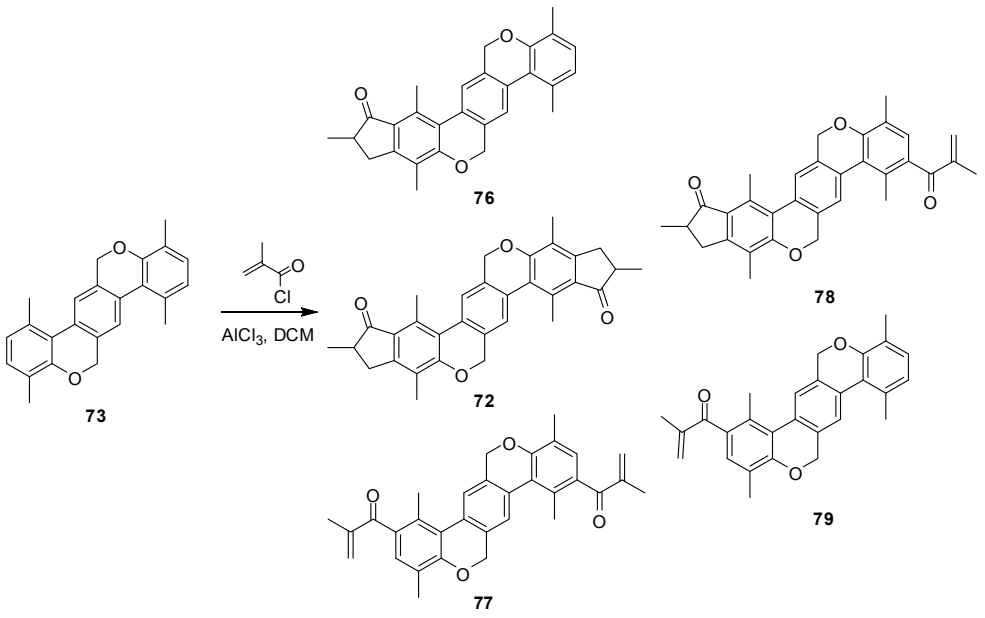

Scheme 22: Preparation of bisketone **72** and identified side products.

The next step is the preparation of the indanone from **73**. Reaction of methacrylic acid in PPA did not proceed and only starting material was recovered, but reaction of methacrylic acid chloride under Friedel-Crafts conditions resulted in a 36% yield of diketone **72**, along with several side-products. Although **72** could be isolated, attempts to optimise this reaction did not result in less complex product mixtures (Scheme 22). Therefore, **73** was reacted with β-chloro-α-methyl propionic acid chloride[38] under Friedel-Crafts conditions to result in **80** as a single regioisomer, in which two diastereomers (*RR*/*SS* and *RS*) could be observed.[39] Direct cyclisation of **80** to **72** with strong acid (H_2SO_4) proceeds in low yield, but elimination to the α,β-unsaturated ketone **81** is preferable. In that case, cyclisation using H_2SO_4 gives the double cyclised product indanone **72** in quantitative yield (Scheme 23).

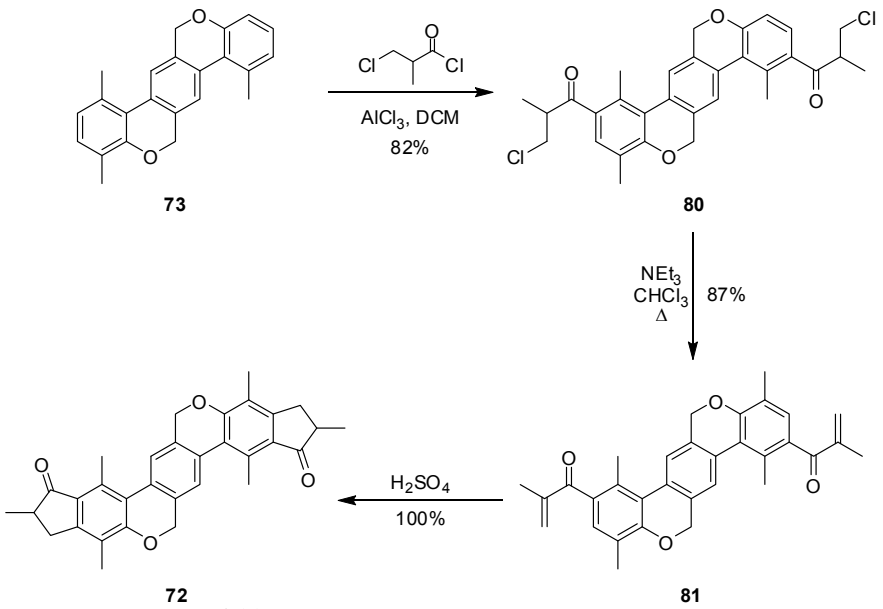

Scheme 23: Preparation of diketone **72**.

Using **72** as starting material, the thioketone **82** prove straightforward to prepare using Laweson's reagent (Scheme 24). Subsequent coupling with diazo-functionalised stator **83** resulted in an episulfide / alkene mixture that was not separated, but directly converted into the diastereomeric mixture **70**. Separation of the diastereomers could be performed using column chromatography to give two compounds, pure racemic (*R,R*)- and (*S,S*)-**70** and the desired compound (*R,S*)-**70**. Preparation of **71** was more challenging. Reaction of thioketone **82** with diazo-functionalised stator **84** resulted in a product mixture, in which both product episulfides were present, as well as substantial quantities of other material. In one instance, filtration, column chromatography and precipitation resulted in a small quantity of pure episulfide, which could be converted to a single diastereomer of molecular double motor **71**. In another instance, filtration of the cooled reaction mixture provided another diastereomer of the intermediate episulfide. Both compounds degrade quickly on silica gel, aluminium oxide and during aqueous workup. However, refluxing these insoluble materials in the presence of excess PPh_3 results in single diasteromers of the product molecular double motors **71**, without degradation under the reaction conditions. Remaining PPh_3 was removed by a published procedure using a Merrifield Resin.[40] Aqueous workup and column chromatography result in degradation of both compounds. However, the poor solubility of the compounds could be used in repetitive precipitation procedures to provide small quantities of the pure alkenes **71**.

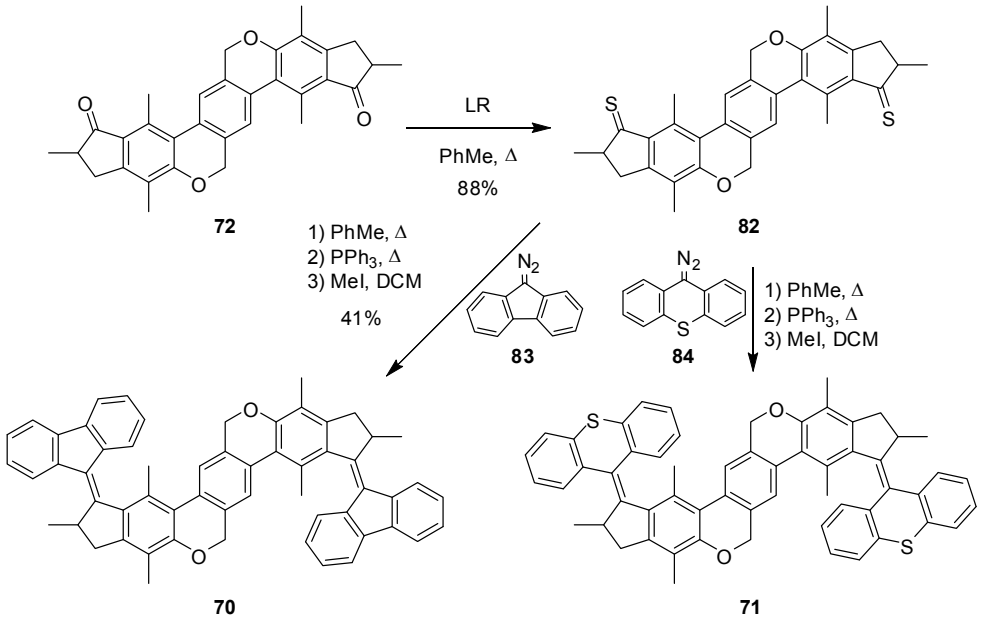

Scheme 24: Double Barton-Kellogg coupling for target structures **71** and **72**.

6.4.3 Identification of diasteromers

The isolated diasteromers of **70** displayed similar ^{1}H NMR-spectra, the major difference being the shift of the central benzo[c]chromene CH_2 (see experimental section). As only one of the two diasteromers can possibly display linear translational motion, correct assignment of the diastereomers is of utmost importance. The point symmetry of both the diastereomers of **70** precluded the use of ^{1}H-COSY and NOESY-spectroscopy to provide evidence as to which one was which. Attempts in this direction did result in well-resolved spectra, but despite the visibility of several NOE interactions, no information on the diastereomeric identity could be retrieved. This is due to the fact that for the *RS*-diastereomer, NOE's are present for the stator aromatic protons with both equatorial CH_2-protons, and this is equally true for the case of the *RR*/*SS*-enantiomeric mixture (Figure 6). In both cases, a distinction between the protons cannot be made because they display equal shielding. Calculation of NMR-spectra of both diastereomers using the programme package Gaussian[41] on optimised structures using a variety of basis sets did not result in clear correspondence with the experimental spectra. Using chiral HPLC however, (AD column, *n*-heptane : IPA = 98 : 2), one of the diastereomers could be resolved into enantiomers (r_F = 7.1 min and 14.8 min), with a small impurity at r_F = 9.8 min (3 %). The other diasteromer gave only one peak at r_F = 9.8 min under the same conditions, with the same UV/Vis-spectrum as observed for the impurity of the other batch. Both UV/Vis-spectra were identical to the ones observed in the photochemical experiments. Using this approach,

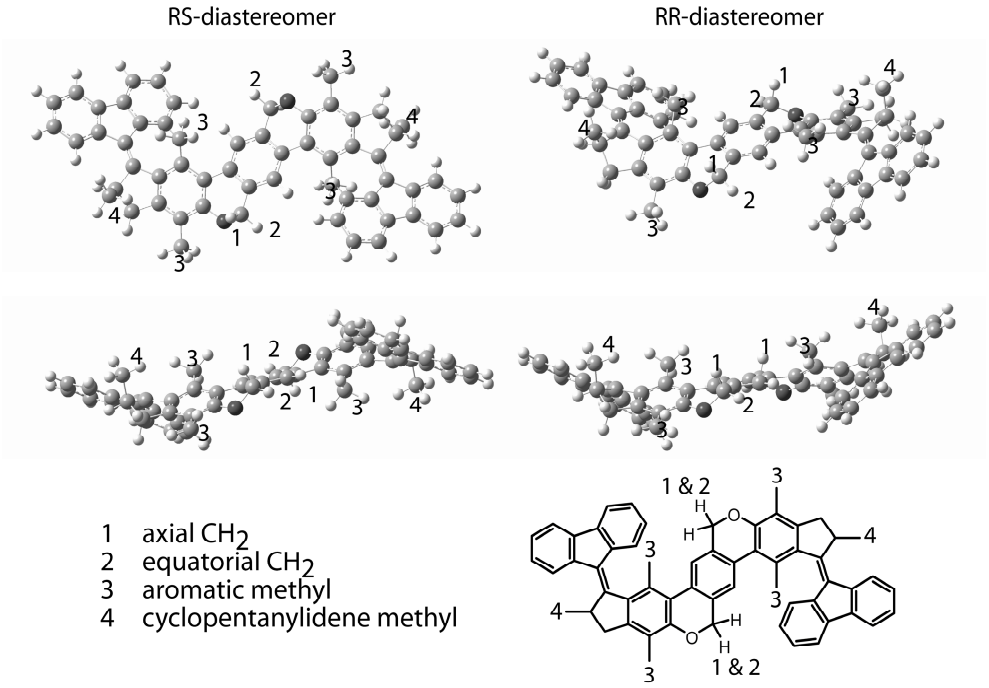

Figure 6: Optimised structures (DFT, B3LYP 6-31G(d,p)) and atomic assignments of (*RS*)-**70** and (*RR*/SS)-**70**. Stereochemical structural formulas can be found in Figure 7.

the diastereomers of **70** were assigned by a combination of ^{1}H NMR- and UV/Vis spectroscopy, in combination with chiral HPLC.

A similar approach was taken for assignment of the diastereomers of **71**. Apparently, degradation in HPLC is slower than on silica gel, and similar to compound **70** one of the diasteromers could be resolved into two enantiomers (AD-column, *n*-heptane : IPA = 98 : 2, r_F = 4.7 and 5.4 min.). The other diastereomer was obtained as a single peak with r_F = 4.3 min. In both cases, the UV/Vis spectra displayed properties similar to those observed in the photochemical experiments.

From the above, it has been made apparent that both **70** and **71** can be obtained as single diastereomers. The (*RR*/SS) enantiomeric mixture generally is more soluble, though in the case of **70**, both compounds can be characterised using standard methods. In the case of (*RS*)-**71**, the poor solubility precludes high enough concentration for ^{13}C and/or APT determination; ^{1}H NMR spectroscopy is possible only using extended pulse sequences.

6.4.4 Photochemical experiments on molecular walkers in solution

The photochemical properties of double motors are somewhat more challenging to study than the properties of single motors. With two axle double bonds present, there exist three possible photochemical outcomes: two-sided double bond isomerisation to result in double-unstable U2, singular double-bond isomerisation to result in a double motor structure one side of which is in the unstable twisted form (US) and finally a compound which is not changed upon irradiation and is the starting compound, S2. Assuming uncorrelated photochemistry, the distribution of the three compounds U2, US and S2 is a function of the theoretical photoequilibrium

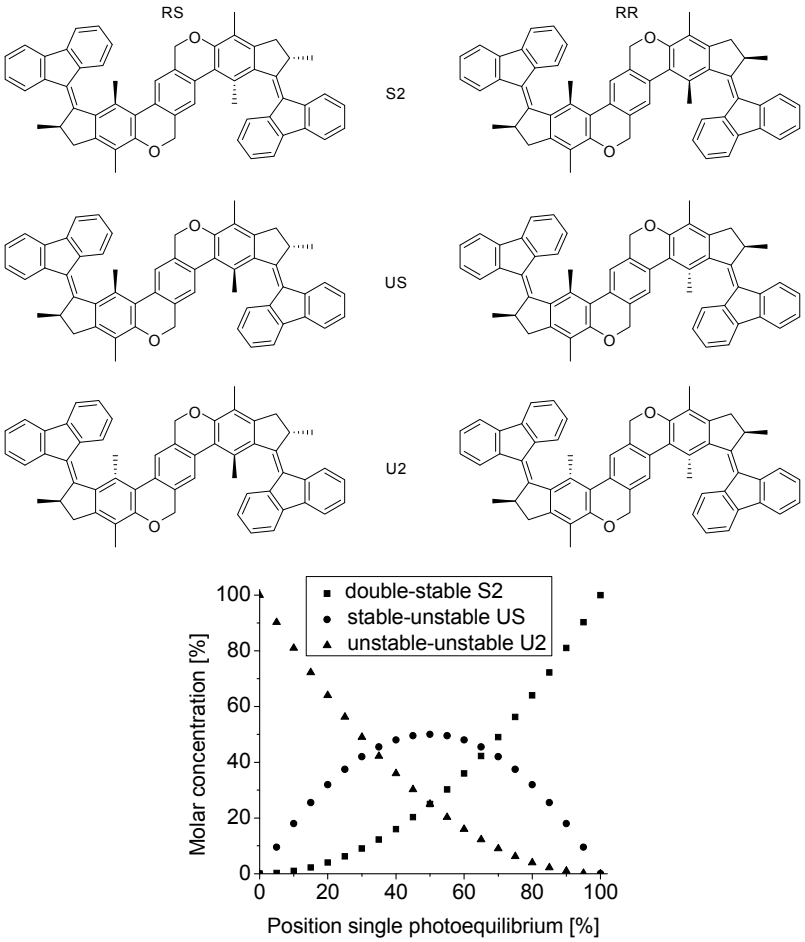

Figure 7: Theoretical molar distribution of the three possible outcomes of the photochemistry of a double motor as a function of the singular double bond photo equilibrium position.

position of a single double bond. For this case, the resulting compound distribution can be calculated (Figure 7). However, the above picture only applies in the case of uncorrelated photochemistry. This condition holds if isomerisation of one of the double bonds has no influence on the rate of the forward and/or reverse photochemical reactions of the other double bond. Because of electronic and the steric factors, as well as change in absorption characteristics of the molecule after the first photochemical reaction, this is hard to imagine. It is more likely to assume some form of correlation between both halves, resulting in a preference for one of the three isomers U2, US or S2.

*UV/Vis spectroscopy of **70***

UV/Vis experiments on the single diasteromer (*RS*)-**70** indicated a clean process with well-defined isosbestic points (Figure 8). Upon irradiation in toluene at -18 °C using 365 nm light, an extra band appeared at λ > 450 nm. The photostationary state was reached in approximately 11 min. Heating of the solution and subsequent cooling resulted in a quantitative return to the original spectrum, indicative of clean photochemistry. Following the thermal process in the temperature range of 10 – 30 °C resulted in the activation parameters according to the approach described in chapter 2: $\Delta^{\ddagger}G^{\circ}_{1}$ = 89.1 kJ mol^{-1}, $\Delta^{\ddagger}H^{\circ}_{1}$ = 83.2 kJ mol^{-1}, $\Delta^{\ddagger}S^{\circ}_{1}$ = -20 J mol^{-1} K^{-1}, k_{Δ}° = 8.0×10^{-4} s^{-1}, Figure 8). The half-life time associated with the process of thermal helix inversion was found to be 14.5 min.

From these experiments several conclusions can be drawn: first of all, there exists strong indication that no significant photodegradation occurs under these conditions, as the restoration of the original UV/Vis-spectrum is complete. It should be added that these experiments could be performed repeatedly using the same sample, strengthening that conclusion. Secondly, the isosbestic point provides indication that if some double unstable form U2 is formed, this is probably not present in significant amounts. This is apparent from the small chance that the US and the U2 form of (*RS*)-**70** have the same absorption characteristics. Previous experiments with similar molecular motors indicate that the extra band that results at > 450 nm upon irradiation is due to the twisted orientation of the stator relative to the rotor (or in this case, the scaffold). As the double unstable form U2 would give rise to a stronger UV/Vis-absorption in this range, it is expected that the absence of a strong band, in combination with the appearance of a clear isosbestic point, is indicative of little conversion, if at all, to the U2 form of (*RS*)-**70**. Finally, it becomes apparent that in comparison to the single motor (refer to chapter 1),[6] a distinct retardation of the process of thermal helix inversion is observed. The $\Delta^{\ddagger}G^{\circ}_{1}$ of 89.1 kJ mol^{-1} is 10 kJ mol^{-1} higher than that reported for the single motor (79.1 kJ/ mol^{-1}). The half-life time for the process rises accordingly, from 15 s to 14.5 min. The regiochemistry of (*RS*)-**70** is

probably the cause of this retardation: with this pattern of substitution, the steric crowding increases dramatically relative to the single motor (refer to Figure 6).

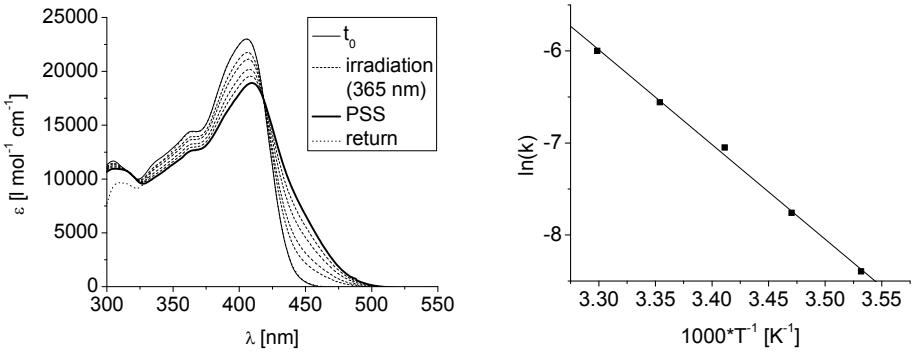

Figure 8**:** Irradiation and thermal conversion of (*RS*)-**70** in toluene at -18 °C, and Arrhenius plot for the process.

UV/Vis experiments on (*RR*/SS)-**70** indicated a similar process with well-defined isosbestic points (Figure 9). Irradiation of (*RR*/SS)-**70** at -18 °C in toluene resulted in a photostationary state in approximately 25 min. Heating of the solution and subsequent cooling resulted in restoration of the original spectrum, indicative of clean photochemistry. The decay process was followed in time at temperatures between 10 and 30 °C to result in rate constants for the process of thermal helix

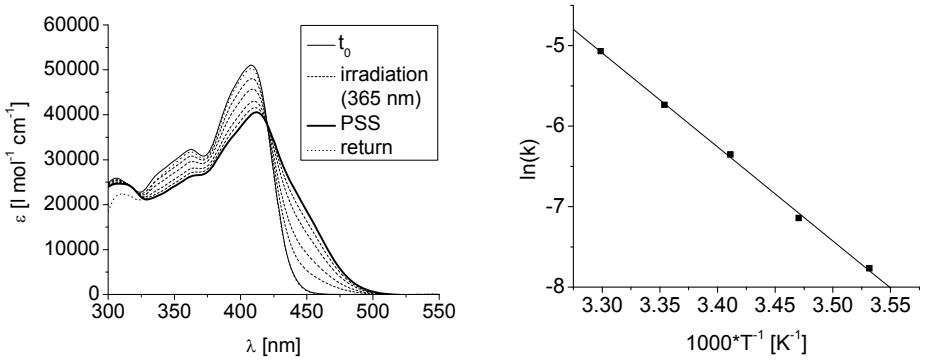

Figure 9: Irradiation and thermal conversion of (*RR*/SS)-**70** in toluene at -18 °C, and Arrhenius plot for the process.

inversion. Standard Eyring and Arrhenius resulted in activation parameters: $\Delta^{\ddagger}G^{o}_{1}$ = 87.3 kJ mol^{-1}, $\Delta^{\ddagger}H^{o}_{1}$ = 94.6 kJ mol^{-1}, $\Delta^{\ddagger}S^{o}_{1}$ = 25 J mol^{-1} K^{-1}, $k_{\Delta}{}^{o}$ = 1.7×10^{-3} s^{-1}. The half-life time for the thermal helix inversion process is calculated from the rate constant to be 6.9 min at room temperature.

The strong similarities between the two diastereomers (*RR*/SS)-**70** and (*RS*)-**70** become apparent from these experiments. UV/Vis spectra of the stable conformations, as well as the change in UV/Vis spectrum upon irradiation follow similar patterns, although the absolute absorption of (*RR*/SS)-**70** is markedly higher. Furthermore, it appears that the thermal process is nearly two times slower for the highly symmetric (*RS*)-**70** in comparison to (*RR*/SS)-**70**. Both compounds display markedly higher barriers for thermal helix inversion than the parent motor, due to the large increase in steric hindrance. Despite the lower absorption at the same wavelength, (*RS*)-**70** appears to display more efficient photochemistry, because the photostationary state is reached in half the time required for (*RR*/SS)-**70** under similar irradiation conditions.

*^{1}H NMR-spectroscopy of **70***

Using ^{1}H NMR spectroscopy, both (*RS*)-**70** and (*RR*/SS)-**70** were subjected to irradiation in toluene–d_8 to verify whether a thermally unstable form could be generated photochemically. For (*RS*)-**70**, irradiation at -20 °C for three hours resulted in a different isomer with cyclopentylidene methyl peaks shifted downfield relative to the starting isomer, and the signals for the aromatic methyl groups split to different chemical shifts (Figure 10). Heating of the sample solution to 45 °C and subsequent cooling restores the original spectrum without observable photodegradation. The presence of a small impurity at 1.3 ppm precludes accurate determination of the integrals, however it is clear that the presence of a significant amount of double unstable form U2 is not likely. This can be seen from the number of aromatic methyl signals between 2.2 and 2.7 ppm, and more clearly by the central CH_2 signals between 4.5 and 5.0 ppm. These display 4 signals for four protons, and other signals are not observed. The ration between S2 and US is estimated to be around 50 : 50.

A similar impurity as observed in (*RS*)-**70** was present in the enantiomeric mixture (*RR*/*SS*)-**70**. For this diastereomer, irradiation resulted in a photo-equilibrium that was shifted further to the side of the unstable form US, and although peaks representing U2 can not be unequivocally assigned, indication of the presence of U2 is given by the relative ratio of the methyl doublets around 1.4 and 1.25 ppm. Four signals are observed for the aromatic methyl peaks. Heating of the sample and subsequent cooling results in a full restoration of the original spectrum, with no observable photodegradation.

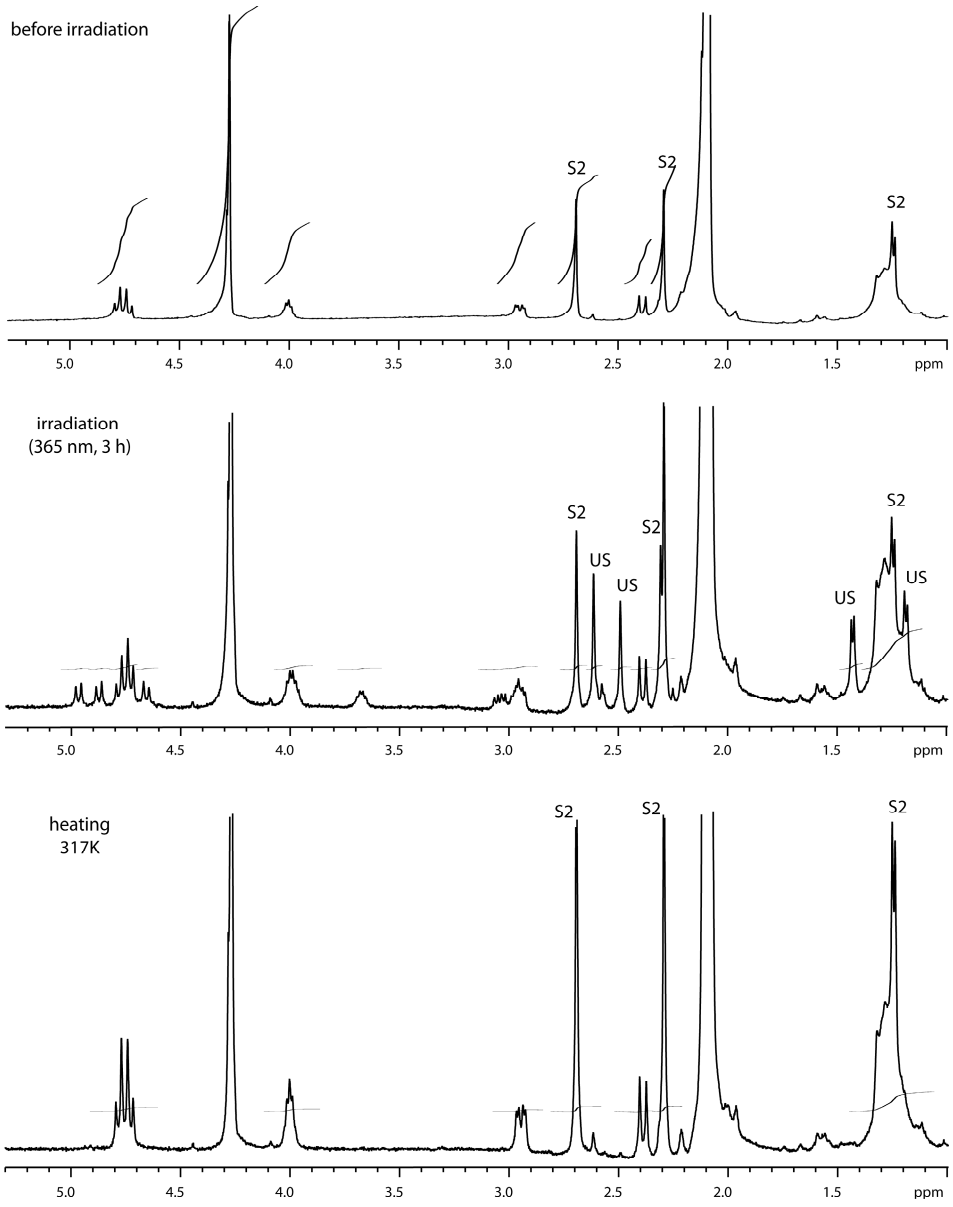

Figure 10: Irradiation and thermal conversion of (*RS*)-**70**.

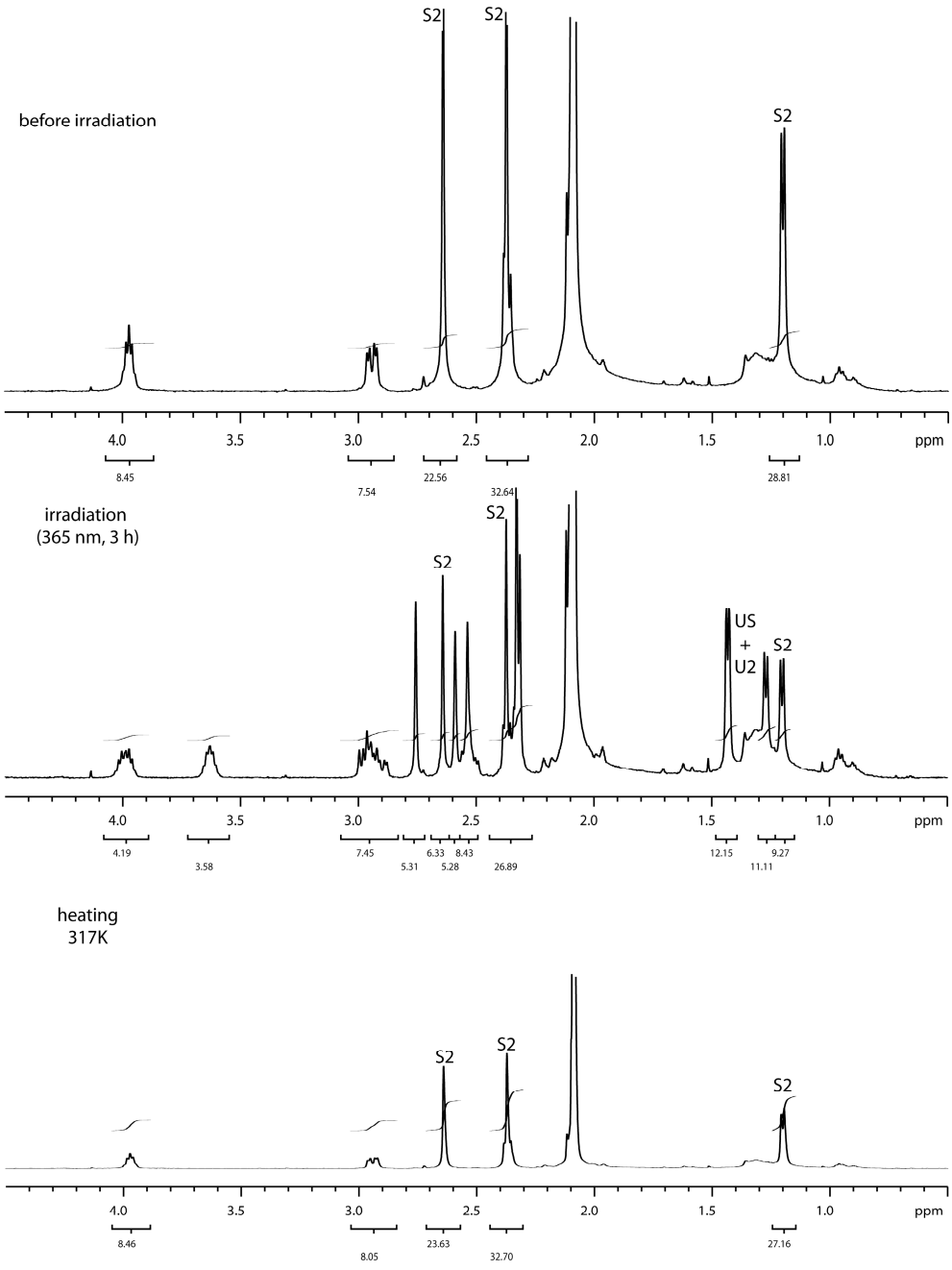

Figure 11: Irradiation and thermal conversion of (*RR*/*SS*)-**70**.

*Fluorescence spectroscopy of **71***

At room temperature, CH_2Cl_2-solutions of (*RR*/SS)-**71** and (*RS*)-**71** were prepared (6.32×10^{-6} and 5.48×10^{-6} M, respectively). The UV/Vis absorption and excitation spectra displayed similar absorption maxima. The emission spectrum displayed maxima of 498 and 508 nm, respectively. Surprisingly, excitation using 488 nm resulted in a similar emission spectrum (λ_{max} = 514 nm), indicative of low absorption at this wavelength. Quantum yields of fluorescence were determined using a protocol from Jorin-Yvon Horiba using perylene and diphenylanthracene standards at 376 nm excitation: (*RR*/*SS*)-**71**: φ_F = 0.14 %, (*RS*)-**71**: φ_F = 0.26 %.[42]

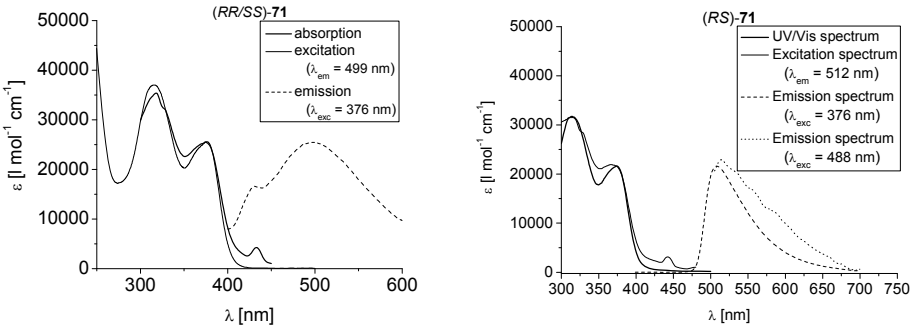

Figure 12: Absorption spectrum and normalised excitation and emission spectra of (*RR*/SS)-**71** (left) and (*RS*)-**71** (right) in DCM.

*UV/Vis spectroscopy of **71***

Using cryogenic techniques similar to those described in chapters 2 and 5, molecular double motor (*RR*/*SS*)-**71** was subjected to photochemical experiments. Upon irradiation with 365 nm light at 115 K in isopentane solution (1.85×10^{-5} M), a small conversion to a thermally unstable form was observed. Following the kinetics at the same temperature resulted in a half-life time of the thermal process of $2.1(1)\times10^2$ s^1 ($k = 3.3(2)\times10^{-3}$ s^{-1}). At higher temperatures (i.e. 120 K) conversion was not high enough to result in meaningful data on the rate of thermal helix inversion (Figure 13) of this structure.

Using propane as a solvent for (*RR*/*SS*)-**71**, irradiation at 115, 110 or 100 K did not result in observable photoconversion. However, at 85 K irradiation resulted in a change of the UV/Vis spectrum, that reverted to the original signal upon heating and cooling to the same temperature. The observation that photochemical conversion at photoequilibrium is higher at temperatures close to the melting point of the solvent

can be explained by the observations made in chapter 5 regarding the effect of viscosity on the photochemistry of molecular motors. It seems that for molecular double motors, the photochemical equilibrium lies quantitatively to the side of the stable isomer at these temperatures, and that the influence of a viscous medium induces increased conversion to the thermally unstable form at photoequilibrium. With this assumption, experiments in the organic-glass forming medium methylcyclohexane – methylcyclopentane were performed at 100 K (3.1×10^5 cP), and indeed considerable photoconversion was observed. An isosbestic point could not be observed. Instead, the shift of the crossing point of the initial spectrum with the spectra resulting from irradiation is indicative of conversion to both the US and U2 forms of (*RR*/*SS*)-**71** (inset Fig 14). However, in solution with normal viscosity, the small change in the UV/Vis absorption prohibited kinetic experiments over a wider temperature range because of the large baseline shifts associated with temperature change, so that no barrier to thermal helix inversion could be determined.

The low solubility of (*RS*)-**71** prevented a similar experimental course. As at room temperature only fractions of the material necessary to reach 10^{-5} M solutions would dissolve in apolar media, high photoconversions are required. For this reason, the same medium as used for (*RR*/*SS*)-**71** was used in the photochemical experiments on (*RS*)-**71**. Although the concentration is unknown under these circumstances, photochemical conversion is observed upon irradiation with 365 nm light in a methylcyclohexane : methylcyclopentane = 1:1 (V/V) organic glass. Heating the solution and subsequent cooling restored the original spectrum. Kinetics experiments

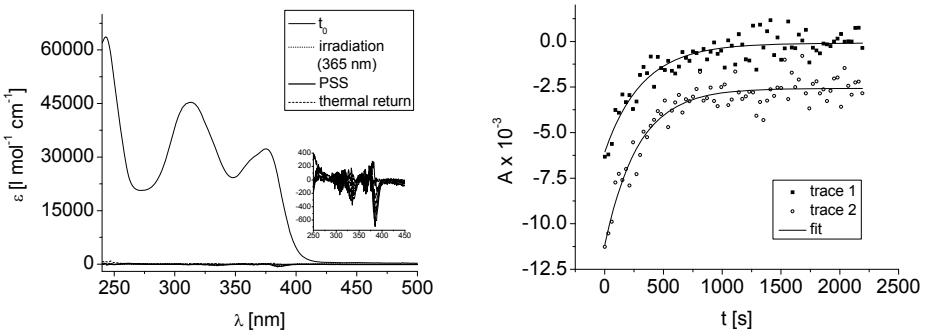

Figure 13: UV/Vis spectrum at room temperature and change in UV/Vis spectrum upon irradiation of (*RR*/*SS*)-**71** with 365 nm light in isopentane solution at 115 K (left), and kinetics of thermal helix inversion (right). Inset: UV/Vis absorbance relative to the full spectrum. The difference spectrum is plotted in the baseline of the UV/Vis spectrum to give an impression of the absolute change in the UV/Vis absorption upon irradiation.

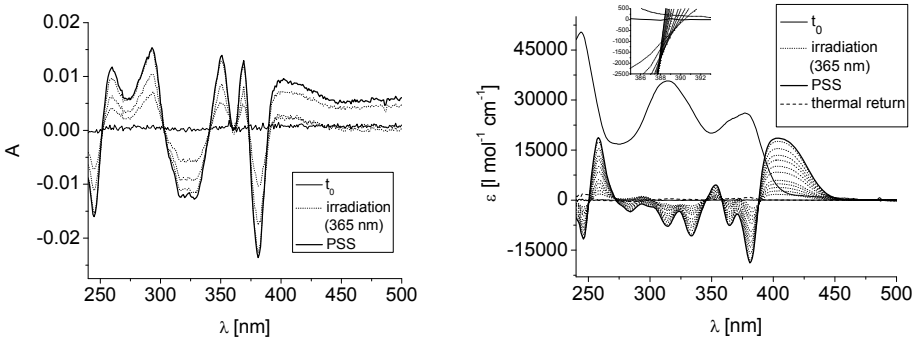

Figure 14: Irradiation of (*RR*/*SS*)-**71** in propane as a UV/Vis difference spectrum (left) and in an organic glass consisting of methylcyclohexane : methylcyclopentane = 1:1 (V/V). The full spectrum was recorded at RT in the same medium, the difference spectrum is plotted in the baseline. Inset: Shift of the crossing point of the initial spectrum and the spectra resulting from irradiation indicative of conversion to the US and U2 forms of (*RR*/*SS*)-**71**.

using low-viscosity media were not attempted for this compound because the expected low photoconversion in combination with the solubility in appropriate apolar media does not allow for accurate determination of rate constants.

From these photochemical experiments, we can conclude that both **70** and **71** display a functioning photochemical – thermal cycle. In case of **70**, this cycle has been characterised in terms of photochemical conversion and thermal helix inversion reaction rates. In case of **71**, the low conversion at photoequilibrium associated with sulphur stators on cyclopentylidene rotors at regular solution viscosity at cryogenic temperatures (chapters 2 and 5) decreases even further, so that it becomes hard to gather data on the unstable form(s). Experiments in organic glasses are indicative of considerable conversion, and in case of (*RR*/*SS*)-**71** the absence of an isosbestic point upon irradiation suggests conversion to both the US and U2 forms of **71** in such media. At regular solution viscosity at temperatures around 100 K, conversion is still present, albeit low.

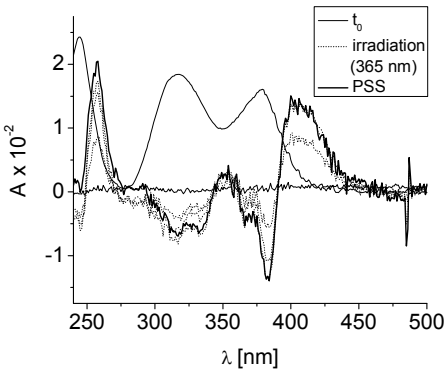

Figure 15: Irradiation of (*RS*)-**71** in an organic glass consisting of methylcyclohexane : methylcyclopentane = 1:1 (V/V) at 100 K (3.1×10^5 cP). The full spectrum was recorded at RT in the same medium.

As quantum yields for *cis* – *trans* isomerisation generally decrease with decreasing temperature, we can assume that at room temperature, there is photochemical *cis* – *trans* isomerisation upon irradiation. This is exemplified by compound **5** from chapter 2 (compound 1 in chapter 5). This compound displays low conversion in normal solution at low temperature (isopentane), but quantitative conversion when applying increased viscosity (chapter 2, figure 19). The PSS for this compound under cryogenic conditions amounts to approximately 30 % unstable at low viscosity, and is nearly quantitative at high viscosity (chapter 5, tables 1 and 2). On the other hand, TA experiments at ambient temperature on the same compound display much higher conversion (chapter 2, figure 21). This indicates that despite low conversion at regular solution viscosity at cryogenic temperatures, conversion at ambient temperature is much higher. Extending this reasoning to compounds **71**, the low conversion to the unstable form(s) observed in cryogenic solution are expected to be much higher in ambient solution. Therefore, as long as the system is kept photochemically rate-limited (see chapter 4), we can assume that unidirectional rotation occurs at a sufficient rate. Data on the position of the equilibrium at room temperature are required to be able to draw conclusions on the rotation behaviour under thermal rate limiting conditions. Unfortunately, obtaining quantitative data is challenging, and as a result data for room temperature behaviour are lacking. Transient absorption (TA) spectroscopy on a μs timescale would provide clear improvement in the experimental setups for the characterisation of the behaviour of these compounds.

For **70**, rates of helix inversion in combination with the photochemical behaviour would allow for translational motion in the order of nm min^{-1}. Such rates are expected to be visible on the timescale of STM experiments. On the other hand, for **71** no data on the thermal behaviour are available. An estimation is possible however by comparison of several related motor structures, which indicates that at room temperature, a rate of thermal helix inversion in the order of a few 100 ns can be expected (Figure 16).

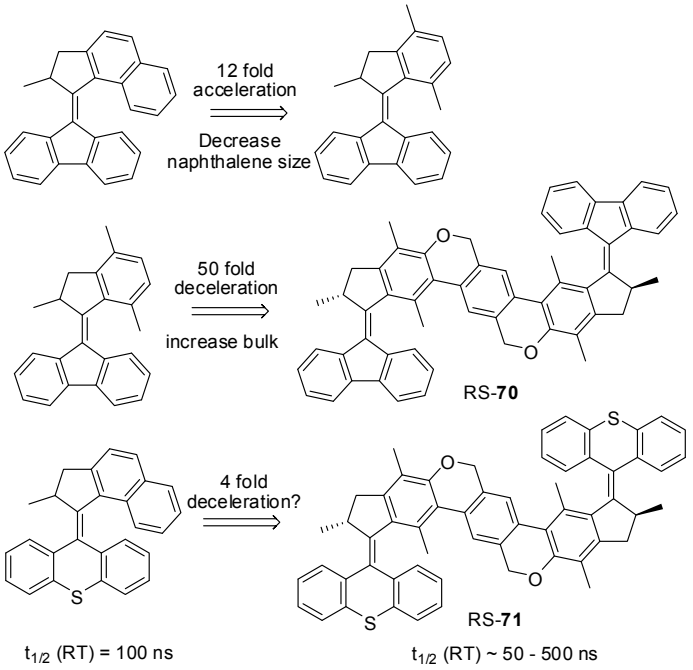

Figure 16: Estimation of the rate of thermal helix inversion of molecular double motor **71**.

Half-life times for thermal helix inversion in this order of magnitude allow for translational motion at considerable pace when the light intensity is high enough. In a system that is close to thermal rate limitation, translational motion in the order of mm/s can be expected if the step size is estimated around 2 nm (2 nm in 400 ns equals 5 mm s^{-1}). However, such rates should be considered the maximum possible rate for translational motion; the actual rate is expected to be lower. Single molecule fluorescence techniques might be able to track motion for these molecules.

6.5 Single molecule spectroscopy on molecular walkers

In collaboration with Johan Visser from our group, STM experiments were performed on compound *RS*-**70**. Using pentacontane on highly oriented graphite (HOPG), single molecules could be detected (Figure 17).[43] The dimensions of the molecule correspond with the dimensions of a single molecule, by comparison with the dimensions of the pentacontane layer. A clear preference for orientation inside the clefts between the pentacontane areas is observed. Dislocation of the molecules was observed both using irradiation and in dark conditions, and as a result no conclusions can be drawn about translational motion induced by rotation of the stators. Further experiments are required to assert conclusions on this matter.

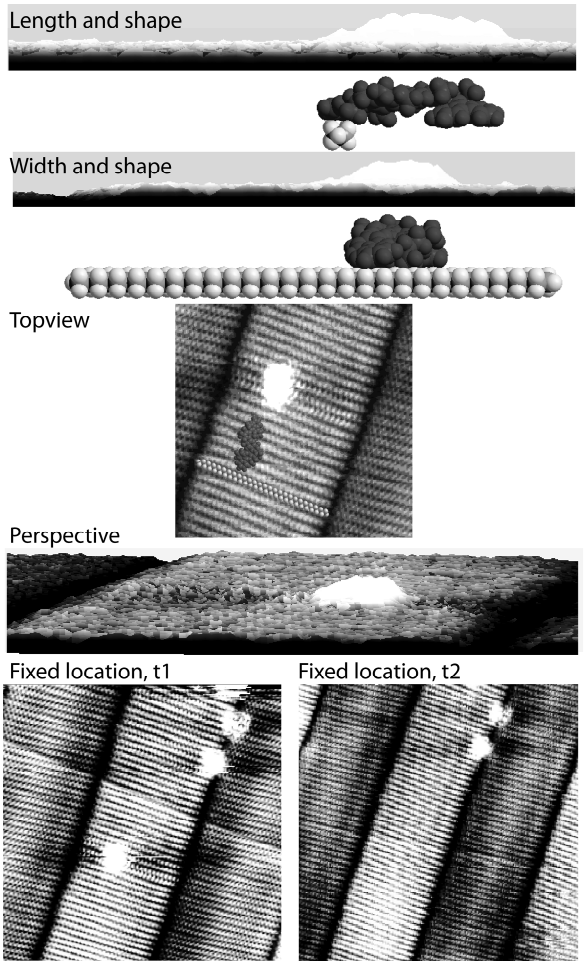

Figure 17: STM-images of *RS*-**70** (courtesy Johan Visser). The bright spot in the middle of the lower left frame was observed to move away for reasons as yet unidentified.

In collaboration with Filippo Lusitani from the Ultrafast Laser and Spectroscopy Laboratory of the University of Groningen widefield single molecule fluorescence spectroscopy experiments were set up to evaluate the possibility of translational motion for *RS*-**71**. A divergent laser beam is used to irradiate an area of micrometer dimensions, and a camera records pictures with adjustable delay times. As a result, one frame is an average over several milliseconds, in which time both multiple *cis-trans* isomerisations and thermal helix inversions can occur (one photochemical – thermal cycle amounts to approximately 400 ns), as well as multiple fluorescence events. When the ratio between these two processes is balanced correctly, translational motion should be visible by recording the fluorescence and evaluating the position of the molecule. In these experiments, the accuracy for the position of the molecule is around 40 nm, but as we are interested in displacements rather than absolute positions, these can be determined with higher accuracy.

Using a spincoating technique (3000 rpm, 180 s) with a 5×10^{-9} M toluene solution of the isomers of **71** on standard glass microscope plates or fresh mica surfaces, single molecules could be observed in real time with widefield fluorescence spectroscopy using 488 nm excitation. (camera frame times 200, 100 and 50 ms, observed area 20×20 μm). In case of (*RR*/*SS*)-**71**, no motion was observed, as anticipated. In contrast, (*RS*)-**71** displayed clearly moving fluorescent dots that represent single molecules (Figure 18). Statistical analysis reveals that motion is not Brownian. However, using shutters a dark experiment could be performed, in which motion could also be observed, which contradicts with the motion being light-driven. Currently, statistical analyses on the direction of motion, the speed of motion and on the dependence of the speed of motion on the irradiation intensity are in progress, as is further identification of the identity of the molecules observed.

Most molecules remain stationary, while only a few display motion. This could be explained by a second photochemical pathway as exemplified in Scheme 19. However, samples do not change their behaviour over time, which is indicative of the thermal reformation of (*RS*)-**71** from this secondary pathway.

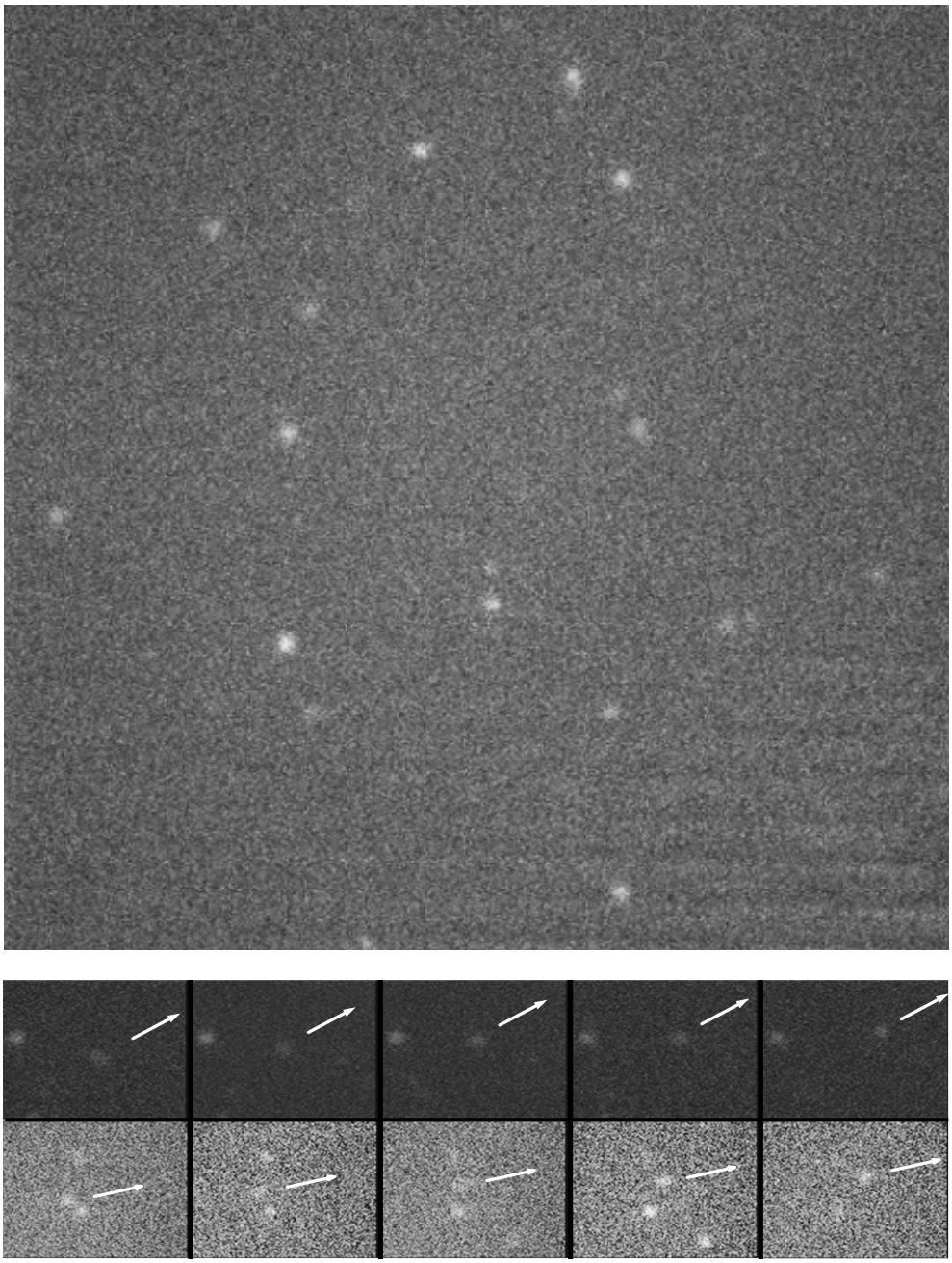

Figure 18: Full-size image of a glass plate spincoated with (*RS*)-**71** (top), and areas of glass plates where moving dots are observed (bottom). Frames are taken at 100 ms delay, 1 pixel equals 40×40 nm).

6.6 Conclusion

Three approaches toward molecular double motors that should be capable of displaying directed linear motion in two dimensions have been explored. Approaches based on a standard naphthalene scaffold failed due to solubility problems, whereas an approach featuring a dibenzo[1,4]dioxin scaffold failed due to potential photochemical degradation. Synthesis of this compound proved possible, however, by the development of a new approach for bisbenzo[1,4]dioxin formation. Despite the relatively low conversion in this reaction, coupling of electron-rich *o*-halophenols is possible using a copper bromide dimethyl sulphide complex. However, even strong steric directive factors cannot prevent Smiles rearrangement, resulting in complex product mixtures.

Molecular double motors configured on a bisbenzo[c]chromene scaffold can be prepared more efficiently, despite the challenges associated with purification in the last steps. It has been shown that such molecular double motors retain the necessary photochemical – thermal cycle, although at low temperature in standard solution, the photoequilibrium lies so far to the side of the stable isomer that observing conversion becomes challenging. However, at ambient temperatures higher conversion is anticipated. Using STM-techniques, single molecules of (*RS*)-**70** were observed, but rotation-induced motion could not be made apparent. Using widefield fluorescence microscopy with spincoated (RS)-**71** on glass- or mica plates, however, motion of fluorescent dots representing single molecules was observed. This could not be repeated with samples of (*RR*/*SS*)-**71** under the same conditions.

6.7 Experimental section

1 9,9'-(2,7-Dimethyl-1,2,6,7-tetrahydrodicyclopenta[a,f]naphthalene-3,8-diylidene)bis(9*H*-thioxanthene)

2 3,8-Di(9*H*-fluoren-9-ylidene)-2,7-dimethyl-1,2,3,6,7,8-hexahydrodicyclopenta[a,f]naphthalene

Bisketone **3** was inserted in a small and dry round-bottomed flask under a nitrogen atmosphere. TBS-hydrazine (3 equivalents) and 5% $Sc(OTf)_3$ were added, and the mixture was heated to 100°C for 3 h. Excess TBS-hydrazine was removed by heating to 60 °C under high vacuum, the resulting oil was quickly examined by ^{1}H NMR to evaluate completion of the reaction, and then dissolved in dry DMF in a dry Schlenk vessel under a nitrogen atmosphere at -50°C. [Bis(trifluoroacetoxy)iodo]benzene (2 eq.) was added, immediately followed by 9*H*-thioxanthene-9-thione or a solution of freshly prepared highly unstable 9*H*-fluorene-9-thione[44] was added (2 eq). The solution was allowed to reach room temperature overnight, resulting in solids appearing in the mixture. These were filtered, and characterised by NMR as being the

impure episulfide in case of reaction with 9*H*-fluorene-9-thione, or a mixture of episulfides and alkenes in the case of 9*H*-thioxanthene-9-thione. Subsequent reaction with PPh_3 in DCM resulted in an insoluble solid which is most likely **1** but could not be characterised, or a small amount of highly insoluble **2** as indicated by low resolution mass spectroscopy and ^{1}H NMR.[45]
2 ^{1}H NMR (400 MHz, $CDCl_3$): δ 7.73 (d, *J* = 7.3 Hz), 7.51 (m), 7.23 (m), 6.98 (m), 6.83 (d, *J* = 8.4 Hz), 6.68 (d, *J* = 8.1 Hz), 6.54 (m), 4.25 (m), 3.45 (dd, *J* = 15.5, 5.5 Hz), 2.44 (d, *J* = 15.4 Hz), 0.78 ppm (d, *J* = 6.6 Hz). MS (EI, %): m/z = 624 (100), 235 (61), 197 (33).

3 2,7-Dimethyl-1,2,6,7-tetrahydrodicyclopenta[a,f]naphthalene-3,8-dione[8]

In a dry nitrogen atmosphere 0.2 g sodium (8.7 mmol) was dissolved in abs EtOH (75 ml) while cooling on an ice bath. 1.85 ml diethylmethylmalonate (10 mmol) in 50 ml EtOH was added and the mixture was stirred for 30 min. From a dripping funnel 0.1 equivalent of 2,6-dibromonaphthalene (0.96 mmol) was added as an EtOH solution, after which the solution was refluxed for 4 h. The resulting mixture was cooled to room temperature and volatiles removed by rotary evaporation. The resulting slurry was poured into water and extracted with dichloromethane, washed with brine, dried over $MgSO_4$ and the solvent evaporated. To this mixture there was added an aqueous 5 M NaOH solution, which was refluxed for 8 h. After cooling the resulting water solution was washed with Et_2O, and H_2SO_4 was added carefully as a 10 M (aq) solution. When foaming had subsided the mixture was refluxed for 5 h, cooled to room temperature and extracted with Et_2O. Washing with water and brine, drying over $MgSO_4$ and evaporation afforded an oily compound, which by NMR was proven to be reasonably pure **8** (153 mg). This was added to a round bottomed flask containing 70 ml PPA at 120°C and mechanically stirred for 4 h. The resulting mixture was cooled to 70°C and poured onto ice, stirred overnight and extracted with EtOAc. Washing with H_2O and brine, drying over $MgSO_4$ and evaporation of the solvent afforded the crude product, which was purified with column chromatography using pentane/EtOAc 8/1 over silicagel to give the pure product as a mixture of *RR*/*SS* and *RS* diastereomers (40 mg) in 22% yield from the dibromide (35 % from the diacid). ^{1}H NMR (400 MHz, $CDCl_3$) δ 9.30 (d, *J* = 8.4 Hz, 2H), 7.61 (d, *J* = 8.4 Hz, 2H), 3.46 (dd, *J* = 17.6, 7.7 Hz, 2H), 2.79 (m, 4H), 1.35 ppm (2*d, 6H). ^{13}C NMR (400 MHz, $CDCl_3$): δ 210.2 (CO), 156.1 (C), 130.9 (CH), 129.9 (C), 128.8 (C), 126.7 (CH), 42.3 (CH), 35.1 (C), 16.5 ppm (CH_3). MS (EI, %): 264 (100), 249 (91), 221 (13), 165 (13). HRMS calcd for $C_{18}H_{16}O_2$: 264.1150, found: 264.1153.

5 2,6-Dimethylnaphthalene[7]

A 3-necked round-bottom flask equiped with reflux condensor and dripping funnel under a dry nitrogen atmosphere was charged with 2.5 g (103 mmol) activated magnesium turnings in 75 ml dry Et_2O. 1.2 eq. of α-chloro-*p*-xylene (123 mmol, 16.3 ml) dissolved in 50 ml Et_2O was added *via* the dripping funnel, followed by 20 min of refluxing to prepare the Grignard reagent. Acetylacetaldehyde dimethyl acetal (17.3 g in 30 ml Et_2O) was added slowly, after which the solution was brought to reflux for 30 min. The resulting solution was poured into a saturated NH_4Cl (aq) solution, and the crude product obtained by extraction with Et_2O and evaporation of the solvent. While cooling on ice, a mixture of H_2SO_4 and H_3PO_4 (125 ml, 3/2 V/V) was added to the resulting black mass under stirring. After 15 min, the cooling bath was removed and the mixture was heated to 65°C for 15 min. The dark coloured mixture was

cooled to room temperature and diluted in water, and then neutralised using aqueous NaOH until pH = 6. Extraction with pentane and subsequent washing, drying and removal of the solvent resulted in the crude product, which was purified by crystallisation from EtOH to yield highly pure 2,6-dimethylnaphthalene (16%). Alternatively, the product can be columned over silicagel using pentane, which results in a higher yield of purified product (6.0 g, 37%). Spectroscopic data were in accordance with those reported.[7]

6 2,6-Bis(bromomethyl)naphthalene[46]

To a 0.05 M solution of 2,6-dimethylnaphtalene **5** in benzene there was added 2.1 eq N-bromosuccinimide. The mixture was irradiated with a Mercury arc lamp for 2 h at ambient temperature, after which the resulting slurry was filtered and solvents removed from the clear solution by rotary evaporation. The pure product was obtained by recrystallisation from chloroform in multiple batches to yield 2,6-di(bromomethyl)naphthalene in 70% yield. Spectroscopic data were in accordance with those reported.[46]

19 6-Bromo-5-hydroxy-2,4,7-trimethylindan-1-one[33]

A quantity of 2.00 g of **39** (5.8 mmol) was dissolved in MeCN (15 ml). Next 3 eq NaI (2.6 g) were added as a MeCN solution, and extra MeCN was added until a clear solution remained. Subsequently 1.5 eq (0.94 g) of TMS-Cl in 8 ml MeCN was added by syringe, and the solution was stirred at room temperature overnight. To the mixture $NaSO_3$ solution was added, and the mixture was extracted with CH_2Cl_2. Washing with brine, drying over $MgSO_4$ and evaporation of the solvent gave 1.51 g of **20** (5.6 mmol, 97%) as a pure yellowish solid. ^{1}H NMR (400 MHz, $CDCl_3$): δ 6.20 (s, 1H), 3.17 (dd, *J* = 17.2, 8.1 Hz, 1H), 2.70 (s, 3H), 2.65 (m, 1H), 2.46 (dd, *J* = 17.0, 4.2 Hz, 1H), 2.22 (s, 3H), 1.27 ppm (d, *J* = 7.3 Hz, 3H). ^{13}C NMR (400 MHz, $CDCl_3$): δ 208.3 (CO), 154.1 (C), 154.0 (C), 137.0 (C), 127.2 (C), 119.1 (C), 114.9 (C), 42.5 (CH), 33.1 (CH_2), 17.2 (CH_3), 16.7 (CH_3), 11.6 ppm (CH_3). MS (EI, %): m/z = 268 (88), 253 (100). HRMS calcd for $C_{12}H_{13}BrO_2$: 268.0098, found: 268.0052.

20 5-Bromo-6-hydroxy-2,4,7-trimethylindan-1-one

Prepared by a similar procedure as compound **19** (96 %). ^{1}H NMR (400 MHz, $CDCl_3$): δ 5.74 (s, 1H), 3.17 (dd , *J* = 16.5, 8.1 Hz, 1H), 2.70 (m, 1H), 2.55 (s, 3H), 2.49 (dd, *J* = 16.7, 3.8 Hz, 1H), 2.32 (s, 3H), 1.27 ppm (d, *J* = 7.3 Hz, 3H). ^{13}C NMR (400 MHz, $CDCl_3$): δ 210.1 (CO), 149.6 (C), 144.6 (C), 133.0 (C), 132.2 (C), 121.9 (C), 120.5 (C), 42.5 (CH), 33.4 (CH_2), 18.5 (CH_3), 16.5 (CH_3), 10.6 ppm (CH_3). MS (EI, %): m/z = 268 (88), 253 (100). HRMS calcd for $C_{11}H_{10}BrO_2$ (M-CH_3): 252.9864, found: 252.9876.

29 1,4,5,8-Tetramethyldibenzo[1,4]dioxin[32]

Reaction of 2-bromo-3,6-dimethylphenol[7] **28** (178 mg, 0.89 mmol) was performed in a dry and nitrogen-flushed Schlenk vessel, charged with $CsCO_3$ (3 eq), pyridine (3 eq) and CuBr·SMe_2 (3 eq) in 20 ml dry MeCN, after which **28** was added. The mixture was brought to reflux, and progress of the reaction was followed with thin layer chromatography (*n*-pentane : diethylether = 25 : 1). Workup could usually be performed within 24 h, after which the solvent was evaporated and the crude product purified using column chromatography on

aluminium oxide to give a white solid (44 mg, 41%). ^{1}H NMR (400 MHz, $CDCl_3$): δ 6.61 (s, 4H), 2.19 ppm (s, 12H). ^{13}C NMR (400 MHz, $CDCl_3$): δ 140.5 (C), 124.1 (CH), 123.1 (C), 14.8 (CH_3). MS (EI, %): m/z = 240 (100), 225 (10), 120 (8).

34 5-Hydroxy-2,4,7-trimethylindan-1-one

In a dry nitrogen atmosphere 1.1 g (5.4 mmol) of **37** was dissolved in 25 ml dry CH_2Cl_2. BBr_3 (2.0 eq., 1 ml) was added, and the mixture was stirred at room temperature overnight. The mixture was poured in water, extracted with EtOAc, washed with brine and dried over $MgSO_4$ to give the crude product as a pure solid (99%), which could be further purified by recrystallisation from $CHCl_3$ to give 0.70 g (67%) of a pure crystalline solid. X-ray crystallography was used to determine the regiochemistry of this compound. ^{1}H NMR (400 MHz, $CDCl_3$): δ 6.68 (s, 1H), 3.21 (dd , *J* = 17.2, 7.7 Hz, 1H), 2.69 (m, 1H), 2.54 (s, 3H), 2.50 (1/2 * dd, *J* = 17.2, 3.7 Hz, 1H), 2.15 (s, 3H), 1.29 ppm (d, *J* = 7.7 Hz, 3H). ^{13}C NMR (400 MHz, $CDCl_3$): δ210.4 (CO), 159.7 (C), 156.4 (C), 138.5 (C), 126.4 (C), 117.9 (C), 117.0 (CH), 42.5 (CH), 33.7 (CH_2), 18.2 (CH_3), 16.9 (CH_3), 10.4 (CH_3). MS (EI, %): m/z = 190 (69), 175 (100). HRMS calcd for $C_{12}H_{14}O_2$: 190.0994, found: 190.1002.

35 6-Hydroxy-2,4,7-trimethylindan-1-one

Prepared by a similar procedure as **34** in 99% yield. ^{1}H NMR (400 MHz, $CDCl_3$): δ 6.92 (s, 1H), 5.59 (bs, 1H), 3.13 (dd, *J* = 16.8, 8.1 Hz, 1H), 2.65 (m, 1H), 2.51 (s, 3H), 2.43 (dd, *J* = 16.8, 3.9 Hz, 1H), 2.22 (s, 3H), 1.27 ppm (d, *J* = 7.7 Hz, 3H). ^{13}C NMR (400 MHz, $CDCl_3$): δ 211..6 (CO), 153.3 (C), 145.6 (C), 134.2 (C), 133.2 (C), 122.4 (CH), 120.2 (C), 42.8 (CH), 32.5 (CH_2), 17.5 (CH_3), 16.6 (CH_3), 9.4 ppm (CH_3). MS (EI, %): m/z = 190 (90), 175 (100), 147 (24). HRMS calcd for $C_{12}H_{14}O_2$: 190.0994, found: 190.0993.

37 5-Methoxy-2,4,7-trimethylindan-1-one and **38** 6-methoxy, 2,4,7-trimethylindan-1-one

PPA was heated to 70°C and 5.0 g 2,5-dimethylphenyl methyl ether (prepared by reaction of 2,5-dimethylphenol with K_2CO_3 and MeI in acetone, 36.7 mmol) was added as a finely powdered solid. Subsequently there was added 3.1 ml methacrylic acid (1.0 eq.) and the mixture was stirred mechanically for 5 h. The black mixture was poured onto ice and stirred overnight, and then extracted with EtOAc. Washing with brine and drying over $MgSO_4$ afforded the crude product, consisting of a 2: 1 mixture of **37** and **38**. After removal of the solvent by rotary evaporation these compounds were separated using column chromatography with heptane-toluene 1:1 to result in pure single isomers, which were assigned by NOESY spectroscopy at this stage and by X-ray crystallography in a later stage. **37**: ^{1}H NMR (400 MHz, $CDCl_3$): δ 6.89 (s, 1H), 3.81 (s, 3H), 3.13 (dd, *J* = 16.6, 8.3 Hz, 1H), 2.64 (m, 1H), 2.48 (s, 3H), 2.43 (dd, *J* = 16.6, 3.9 Hz, 1H), 2.27 (s, 3H), 1.26 ppm (d, *J* = 7.3 Hz, 3H). ^{13}C NMR (400 MHz, $CDCl_3$): δ 211.2 (CO), 156.8 (C), 144.3 (C), 134.0 (C), 132.7 (C), 123.9 (C), 117.7 (CH), 56.2 (CH_3), 42.7 (CH), 32.4 (CH_2), 17.8 (CH_3), 16.5 (CH_3), 9.6 ppm (CH_3). MS (EI, %): m/z = 204 (100), 189 (92), 161 (35). HRMS calcd for $C_{13}H_{16}O_2$: 204.1150, found: 204.1141. **38**: ^{1}H NMR (400 MHz, $CDCl_3$): δ 6.58 (s, 1H), 3.86 (s, 3H), 3.18 (dd, *J* = 17.1, 8.1 Hz, 1H), 2.62 (m, 1H), 2.59 (s, 3H), 2.47 (dd, *J* = 17.1, 3.8 Hz, 1H), 2.08 (s, 3H), 1.26 (d, *J* = 7.6 Hz, 3H). ^{13}C NMR (400 MHz, $CDCl_3$): δ 209.2 (CO), 161.6

(C), 154.4 (C), 138.1 (C), 126.4 (C), 119.9 (C), 111.5 (CH), 55.7 (CH_3), 42.3 (CH), 33.4 (CH_2), 18.4 (CH_3), 16.7 (CH_3), 10.5 ppm (CH_3). MS (EI, %): m/z = 204 (80), 189 (100), 161 (12). HRMS calcd for $C_{13}H_{16}O_2$: 204.1150, found: 204.1142.

39 2,6-Dibromo-5-hydroxy-2,4,7-trimethylindan-1-one

A round-bottomed flask was charged with 1.79 g (9.4 mmol) **34** in 150 ml CH_2Cl_2. Bromine (5.0 eq, 2.4 ml) and a small crystal of iodine were added, and the mixture was stirred at room temperature overnight. Aqueous $NaSO_3$ was added, after which the layers were separated. Extraction with CH_2Cl_2, washing with brine, drying over $MgSO_4$ and removal of the solvent by rotary evaporation afforded a 3.19 g (9.2 mmol, 97%) of a brownish solid, which turned out to be pure **39**. ^{1}H NMR (400 MHz, $CDCl_3$): δ 6.34 (s, 1H), 3.63 (d, *J* = 18.3 Hz, 1H), 3.24 (d, *J* = 18.3 Hz, 1H), 2.72 (s, 3H), 2.19 (s, 3H), 1.92 ppm (s, 3H). ^{13}C NMR (400 MHz, $CDCl_3$): δ 199.2 (CO), 155.3 (C), 149.6 (C), 138.8 (C), 123.4 (C), 119.2 (C), 115.4 (C), 60.4 (C), 44.4 (CH_2), 27.3 (CH_3), 17.5 (CH_3), 11.7 ppm (CH_3). MS (EI, %): m/z = 348 (31), 267 (100), 239 (12). HRMS calcd for $C_{12}H_{12}O_2{}^{81}Br_2$: 349.9163, found: 349.9166.

40 2,5-Dibromo-6-hydroxy-2,4,7-trimethylindan-1-one

Prepared by a similar procedure as **39** (91%). ^{1}H NMR (400 MHz, $CDCl_3$): δ 5.79 (s, 1H), 3.62 (d, *J* = 18.0 Hz, 1H), 3.28 (d, *J* = 17.6 Hz, 1H), 2.58 (s, 3H), 2.31 (s, 3H), 1.66 ppm (s, 3H). ^{13}C NMR (400 MHz, $CDCl_3$): δ 200.7 (CO), 150.3 (C), 139.9 (C), 132.3 (C), 129.6 (C), 123.6 (C), 121.6 (C), 60.2 (C), 44.7 (CH_2), 26.9 (CH_3), 18.5 (CH_3), 10.9 ppm (CH_3). MS (EI, %): m/z = 348 (26), 267 (100), 188 (56). HRMS calcd for $C_{12}H_{12}O_2Br_2$: 345.9203, found: 345.9187.

41 6-Bromo-5-(methoxymethoxy)-2,4,7-trimethylindan-1-one

A quantity of 481 mg of **19** (1.8 mmol) was dissolved in 40 ml acetone while stirring. An excess of K_2CO_3 and 1 eq MOM-Cl (0.14 ml) were added, and the mixture was stirred at room temperature overnight. The mixture was diluted with water, extracted with CH_2Cl_2, washed with brine, dried over $MgSO_4$ and the solvents evaporated to give 542 mg (97%) of pure **41** as a yellow oil, which solidified upon standing. ^{1}H NMR (400 MHz, $CDCl_3$): δ 5.09 (s, 2H), 3.64 (s, 3H), 3.17 (dd , *J* = 17.2, 8.1 Hz, 1H), 2.69 (s, 3H), 2.67 (m, 1H), 2.46 (dd, *J* = 17.2, 4.0 Hz, 1H), 2.27 (s, 3H), 1.27 ppm (d, *J* = 7.7 Hz, 3H). ^{13}C NMR (400 MHz, $CDCl_3$): δ 208.4 (CO), 157.1 (C), 153.8 (C), 137.9 (C), 130.7 (C), 127.5 (C), 121.4 (C), 99.8 (CH_2), 57.9 (CH_3), 42.6 (CH), 33.3 (CH_2), 17.2 (CH_3), 16.5 (CH_3), 12.5 ppm (CH_3). MS (EI, %): m/z = 312 (100), 282 (27). HRMS calcd for $C_{14}H_{17}BrO_3$: 312.0361, found: 312.0357.

42 5-Bromo-6-(methoxymethoxy)-2,4,7-trimethylindan-1-one

Prepared by a similar procedure as **41** (99%). ^{1}H NMR (400 MHz, $CDCl_3$): δ 4.96 (s, 2H), 3.58 (s, 3H), 3.17 (dd, *J* = 16.9, 7.8 Hz, 1H), 2.59 (m, 1H), 2.55 (s, 3H), 2.47 (dd, *J* = 16.9, 4.0 Hz, 1H), 2.30 (s, 3H), 1.22 ppm (d, *J* = 7.3 Hz, 3H). ^{13}C NMR (400 MHz, $CDCl_3$): δ 209.0 (CO), 157.1 (C), 152.4 (C), 149.0 (C), 133.8 (C), 130.0 (C), 127.6 (C), 99.6 (CH_2), 57.7 (CH_3), 42.4 (CH), 33.7 (CH_2), 18.4 (CH_3), 16.2 (CH_3), 11.5 ppm (CH_3).

MS (EI, %): m/z = 314 (99), 312 (100), 284 (36), 282 (40), 269 (27), 267 (30). HRMS calcd for $C_{14}H_{17}BrO_3$: 312.0361, found: 312.0365.

49 Dispiro[6-bromo-5-(methoxymethoxy)-2,4,7-trimethylindene-1,2'-thiirane-3',9''-(9''*H*-xanthene)]

In a dry nitrogen atmosphere 257 mg **41** (0.82 mmol) was reacted with 3 eq. TBS-hydrazine and 5% $Sc(OTf)_3$ at 60°C overnight. ^{1}H NMR was used to follow the reaction. When the reaction was complete, the excess hydrazine was removed under high vacuum at 70°C. The product, stable in a pure form under nitrogen in the fridge but not in solution, was deprotected using TBAF in dry THF to result in the even more unstable impure free hydrazone **45**. This compound degraded completely within a few days under any circumstances. It was crystallised overnight using slow evaporation of pentane into EtOAc in the fridge, and the solvents were removed to result in 120 mg (0.37 mmol, 45%) of reasonably pure hydrazone **45**. Without delay, this quantity was added to 8 ml dry DMF and the solution cooled to -50°C. [Bis(acetoxyiodo)]benzene (118 mg, 1 eq) was added, and subsequently 84 mg (1 eq) of 9*H*-thioxanthene-9-thione **12** was added as a pre-cooled CH_2Cl_2-DMF solution. The solution was allowed to reach room temperature overnight, and DCM (50 ml) was added. The solution was washed thoroughly with water and brine, dried over $MgSO_4$ and the solvents evaporated to give the crude product, which was purified by column chromatography using pentane/EtOAc to give 111 mg of **49** as a pure yellow oil (0.21 mmol, 57% from the hydrazone). ^{1}H NMR (400 MHz, CD_2Cl_2): δ 7.79 (d, *J* = 8.1 Hz, 1H), 7.65 (d, *J* = 7.7 Hz, 1H), 7.46 (d, *J* = 7.7 Hz, 1H), 7.30 (t, *J* = 7.3 Hz, 1H), 7.23 (m, 3H), 7.11 (t, *J* = 7.3 Hz, 1H), 4.92 (m, 2H), 3.54 (s, 3H), 3.06 (dd, *J* = 15.8, 6.6 Hz, 1H), 2.27 (s, 3H), 2.19 (d, *J* = 15.4 Hz, 1H), 2.14 (s, 3H), 1.43 (m, 1H), 1.01 ppm (d, *J* = 7.0 Hz, 3H). ^{13}C NMR (400 MHz, CD_2Cl_2): δ 152.7 (C), 144.3 (C), 139.2 (C), 136.7 (C), 136.3 (C), 135.3 (C), 134.6 (C), 132.3 (C), 130.9 (CH), 129.1 (CH), 127.3 (CH), 127.3 (CH), 127.2 (CH), 126.9 (C), 126.8 (CH), 126.1 (CH), 120.2 (C), 99.8 (CH_2), 71.6 (CS), 62.7 (CS), 58.1 (CH_3), 40.8 (CH), 36.5 (CH_2), 21.7 (CH_3), 19.5 (CH_3), 13.4 (CH_3). MS (EI, %): m/z = 526 (87), , 481 (37), 447 (11), 197 (100). HRMS calcd for $C_{27}H_{25}BrO_2S_2$: 524.0479, found: 524.0452.

50 Dispiro[5-bromo-6-(methoxymethoxy)-2,4,7-trimethylindene-1,2'-thiirane-3',9''-(9''*H*-xanthene)]

Prepared by a similar procedure as **49** (32% from the ketone). ^{1}H NMR (400 MHz, CD_2Cl_2): δ 7.79 (d, *J* = 8.1 Hz, 1H), 7.65 (d, *J* = 7.7 Hz, 1H), 7.46 (d, *J* = 7.7 Hz, 1H), 7.30 (t, *J* = 7.3 Hz, 1H), 7.23 (m, 3H), 7.11 (t, *J* = 7.3 Hz, 1H), 4.92 (m, 2H), 3.54 (s, 3H), 3.06 (dd, *J* = 15.8, 6.6 Hz, 1H), 2.27 (s, 3H), 2.19 (d, *J* = 15.4 Hz, 1H), 2.14 (s, 3H), 1.43 (m, 1H), 1.01 ppm (d, *J* = 7.0 Hz, 3H). ^{13}C NMR (400 MHz, CD_2Cl_2): δ 152.7 (C), 144.3 (C), 139.2 (C), 136.7 (C), 136.3 (C), 135.3 (C), 134.6 (C), 132.3 (C), 130.9 (CH), 129.1 (CH), 127.3 (CH), 127.3 (CH), 127.2 (CH), 126.9 (C), 126.8 (CH), 126.1 (CH), 120.2 (C), 99.8 (CH_2), 71.6 (CS), 62.7 (CS), 58.1 (CH_3), 40.8 (CH), 36.5 (CH_2), 21.7 (CH_3), 19.5 (CH_3), 13.4 (CH_3). MS (EI, %): m/z = 526 (87), , 481 (37), 447 (11), 197 (100). HRMS calcd for $C_{27}H_{25}BrO_2S_2$: 524.0479, found: 524.0459.

51 9-(6-Bromo-5-(methoxymethoxy)-2,4,7-trimethylinden-1-ylidene)-9*H*-thioxanthene

A toluene solution of 110 mg **49** (0.21 mmol) and an excess of PPh_3 was heated at reflux overnight. Toluene was evaporated and there was added CH_2Cl_2 with excess MeI to destroy remaining PPh_3. The remaining solution was filtered over silicagel and evaporated to give a mixture of the crude product and triphenylphosphine sulphide. The alkene was isolated by column chromatography using toluene to result in 90 mg (0.18 mmol, 86 %) of the pure alkene as a white solid. ^{1}H NMR (400 MHz, CD_2Cl_2): δ 8.03 (dd, *J* = 7.7, 0.7 Hz, 1H), 7.84 (dd, *J* = 7.7, 1.5 Hz, 1H), 7.80 (dd, *J* = 7.7, 0.7 Hz, 1H), 7.60 (dt, *J* = 7.7, 1.1 Hz, 1H), 7.48 (dt, *J* = 7.5, 1.5 Hz, 1H), 7.43 (dt, *J* = 7.3, 1.5 Hz, 1H), 7.33 (dt, *J* = 7.7, 1.1 Hz, 1H), 7.26 (dd, *J* = 7.7, 1.5 Hz, 1H), 5.58 (m, 2H), 4.44 (q, *J* = 6.6 Hz, 1H), 3.91 (s, 3H), 3.58 (dd, *J* = 15.6, 6.4 Hz, 1H), 2.73 (d, *J* = 5.4 Hz, 1H), 1.57 (s, 3H), 0.96 ppm (d, *J* = 7.0 Hz, 3H). ^{13}C NMR (400 MHz, CD_2Cl_2): δ 153.2 (C), 146.3 (C), 146.0 (C), 140.9 (C), 137.7 (C), 136.4 (C), 136.3 (C), 135.8 (C), 134.2 (C), 129.4 (C), 128.2 (CH), 128.1 (CH), 128.0 (CH), 127.8 (CH), 127.0 (C), 126.9 (CH), 126.7 (CH), 126.7 (CH), 126.4 (CH), 119.9 (C), 100.1 (CH_2), 58.0 (CH_3), 38.4 (CH_2), 37.6 (CH), 21.6 (CH_3), 19.2 (CH_3), 13.6 (CH_3). MS (EI, %): m/z = 494 (37), 449 (100). HRMS calcd for $C_{27}H_{25}BrO_2S$: 492.0758, found: 492.0739.

52 9-(5-Bromo-6-(methoxymethoxy)-2,4,7-trimethylinden-1-ylidene)-9*H*-thioxanthene

Prepared by a similar procedure as **52** (90 %). ^{1}H NMR (400 MHz, $CDCl_3$): δ 7.74 (d, *J* = 7.7 Hz, 1H), 7.55 (d, *J* = 7.7 Hz, 1H), 7.51 (dd, *J* = 7.7, 0.7 Hz, 1H), 7.29 (t, *J* = 7.7 Hz, 1H), 7.17 (m, 3H), 7.01 (m, 1H), 4.82 (m, 2H), 4.15 (m, 1H), 3.54 (s, 3H), 3.34 (dd, *J* = 15.0, 6.2 Hz, 1H), 2.48 (d, *J* = 5.0 Hz, 1H), 2.35 (s, 3H), 1.17 (s, 3H), 0.69 ppm (d, *J* = 7.0 Hz, 3H). ^{13}C NMR (400 MHz, $CDCl_3$): δ 152.1 (C), 145.7 (C), 141.7 (C), 140.4 (C), 139.3 (C), 137.2 (C), 136.0 (C), 135.2 (C), 132.4 (C), 129.6 (C), 128.0 (C), 128.0 (CH), 127.9 (CH), 127.6 (CH), 127.2 (CH), 126.3 (2*CH), 126.3 (CH), 126.1 (CH), 120.2 (C), 99.1 (CH_2), 57.8 (CH_3), 38.8 (CH_2), 37.1 (CH), 19.5 (CH_3), 19.2 (CH_3), 15.1 (CH_3). MS (EI, %): m/z = 494 (100), 449 (92), 235 (63), 197 (41). HRMS calcd for $C_{27}H_{25}BrO_2S$: 492.0758, found: 492.0749.

53 9-(6-Bromo-5-hydroxy-2,4,7-trimethylinden-1-ylidene)-9*H*-thioxanthene

In a dry nitrogen atmosphere 10 ml dry CH_2Cl_2 and 200 µl TFA were stirred at room temperature. Compound **51** (22 mg, 45 µmol) was added, and the reaction was followed by TLC until completion (usually < 2 h). EtOAc and H_2O were added, and subsequently 0.5 ml conc. $NaHCO_3$ (aq) was added. Very quickly, the layers were separated, and the organic phase was washed once with brine as quick as possible. Drying with $MgSO_4$ and evaporation of the solvents gave double-bond shifted product(s) as well as the product phenol. The latter was crystallised from Et_2O to result in 14 mg (67% after one crystallisation) pure **53** as a clear crystalline compound. As long as it is kept dry (as a solid or in solution) the compound is stable. ^{1}H NMR (400 MHz, $CDCl_3$): δ7.71 (d, *J* = 7.7 Hz, 1H), 7.54 (d, *J* = 7.7 Hz, 1H), 7.49 (d, *J* = 7.7 Hz, 1H), 7.28 (t, *J* = 7.5 Hz, 1H), 7.13 (m, 2H), 7.01 (m, 2H), 5.70 (bs, 1H), 4.15 (m, 1H), 3.27 (dd, *J* = 15.5, 6.4 Hz, 1H), 2.45 (d, *J* = 5.4 Hz, 1H), 2.23 (s, 3H), 1.27 (s, 3H), 0.69 ppm (d, *J* = 7.0 Hz, 3H). ^{13}C NMR (400 MHz, $CDCl_3$): δ 150.0 (C), 146.0 (C), 145.6 (C), 140.8 (C), 137.5 (C), 136.1 (C), 135.6 (C), 132.6 (C), 131.9 (C), 128.0 (C), 127.9 (CH), 127.8 (CH), 127.7 (CH), 127.4 (CH), 126.5 (CH), 126.3 (CH), 126.2 (CH),

125.9 (CH), 118.6 (C), 113.0 (C), 38.0 (CH_2), 37.2 (CH), 21.2 (CH_3), 19.3 (CH_3), 12.7 (CH_3). MS (EI, %): m/z = 448 (70), 433 (22), 235 (100). HRMS calcd for $C_{25}H_{21}BrOS$: 448.0496, found: 448.0487.

55 9-(5-Bromo-6-hydroxy-2,4,7-trimethylinden-1-ylidene)-9*H*-thioxanthene

In a dry nitrogen atmosphere 4.5 ml dry CH_2Cl_2 and 0.1 ml TFA were stirred at room temperature. 13 mg (26 μmol) **52** was added, and the reaction was followed by TLC until completion (< 1 h). EtOAc and H_2O were added, and subsequently 1 ml conc. $NaHCO_3$ (aq) was added. Very quickly, the layers were separated, and the organic phase was washed once with brine as quick as possible. Drying with $MgSO_4$ and evaporation gives the free phenol **55** as a light-purple solid (8.5 mg, 72%). ^{1}H NMR (400 MHz, CH_2Cl_2): δ7.77 (d, *J* = 7.7 Hz, 1H,), 7.58 (dd, *J* = 7.7, 1.1 Hz, 1H), 7.52 (d, *J* = 8.1, 1.1 Hz, 1H), 7.33 (t, *J* = 7.7 Hz, 1H), 7.21 (t, *J* = 7.7 Hz, 1H), 7.16 (t, J = 7.7 Hz, 1H), 7.07 – 6.99 (m, 2H), 5.44 (bs, 1H), 4.17 (m, 1H), 3.36 (dd, *J* = 15.0, 6.2 Hz, 1H), 2.48 (d, *J* = 15.0 Hz, 1H), 2.35 (s, 3H), 1.17 (s, 3H), 0.69 ppm (d, *J* = 6.6 Hz, 3H). ^{13}C NMR (400 MHz, CH_2Cl_2): 149.6 (C), 146.2 (C), 141.0 (C), 139.2 (C), 137.9 (C), 137.8 (C), 136.4 (C), 135.7 (C), 131.4 (C), 129.9 (C), 128.2 (CH), 128.1 (CH), 128.0 (CH), 127.8 (CH), 126.9 (CH), 126.7 (CH), 126.7 (CH), 126.4 (CH), 120.7 (C), 113.5 (C), 38.7 (CH_2), 37.6 (CH), 19.4(CH_3), 19.3 (CH_3), 14.3 (CH_3). MS (EI, %): m/z = 450 (41), 448 (36), 235 (100). HRMS calcd for $C_{25}H_{21}{}^{81}BrOS$: 450.0476, found: 450.0463.

70 Bisbenzo[c]chromene-fluorene double motor (BCF)

In a dry nitrogen atmosphere, 27 mg of the bisthioketone **82** was brought to reflux in toluene. In portions there was added 4 eq. of diazofluorene **83** as a PhMe solution over approximately 3 h, and reflux was continued for 2 h. After evaporation of the solvent, separation of the mixture of bisfluorene, *RR*/SS racemate and the *RS*-(meso) diastereomer was possible by column chromatography using pentane : chloroform = 2 : 1 in combination with crystallisation (PhMe, preferential crystallisation of the *RS* diastereomer). The diastereomers were assigned on the basis of the central CH_2 proton shifts and by polarity and symmetry considerations, which was verified by chiral HPLC analysis (AD-column, heptane : isopropanol = 98 : 2). Maldi-mass spectrometry was performed on a pure diastereomeric mixture. The total product yield after isolation was 41%, part of which as a mixture of diasteromers. *RR*/SS diastereomer: ^{1}H NMR (500 MHz, CD_2Cl_2): δ 7.93 (m, 6H), 7.73 (m, 4H), 7.37 (m, 4H), 7.23 (m, 4H), 5.23 (d, *J* = 12.5 Hz, 2H), 5.02 (d, *J* = 12.5 Hz, 2H), 4.17 (m, 2H), 3.29 (dd, *J* = 14.8, 5.7 Hz, 2H), 2.71 (d, *J* = 15.4 Hz, 2H), 2.59 (s, 6H), 2.30 (s, 6H), 1.36 ppm (d, *J* = 6.6 Hz, 6H). ^{13}C NMR (500 MHz, CD_2Cl_2): 155.5 (C), 152.3 (C), 146.8 (C), 139.7 (C), 139.6 (C), 139.6 (C), 138.0 (C), 135.7 (C), 132.8 (C), 132.3 (C), 130.0 (C), 129.9 (C), 127.1 (CH), 126.9 (CH), 126.7 (CH), 126.5 (CH), 123.8 (CH), 123.3 (CH), 123.1 (CH), 122.9 (C), 121.4 (C), 119.7 (CH), 119.4 (CH), 69.8 (CH_2), 43.6 (CH), 40.3 (CH_2), 22.4 (CH_3), 19.1 (CH_3), 12.4 ppm (CH_3). MS (Maldi, α-cyano-4-hydroxycinnamic acid) calcd for $C_{58}H_{46}O_2$: 775.0, found: 774.7. *RS*-diastereomer: ^{1}H NMR (500 MHz, CD_2Cl_2): δ 7.94 (m, 2H), 7.84 (m, 4H), 7.76 (s, 2H), 7.62 (d, *J* = 8.1 Hz, 2H), 7.35 (m, 4H), 7.20 (t, *J* = 7.7 Hz, 2H), 5.16 (d, J = 12.5 Hz, 2H) 5.09 (d, *J* = 12.8 Hz, 2H), 4.17 (m, 2H), 3.27 (dd, *J* = 15.0, 6.2 Hz, 2H), 2.70 (d, *J* = 15.4

Hz, 2H), 2.66 (s, 6H), 2.28 (s, 6H), 1.39 ppm (d, *J* = 6.6 Hz, 6H). ^{13}C NMR (500 MHz, $CDCl_3$): 155.8 (C), 152.5 (C), 146.8 (C), 139.7 (C), 139.7 (C), 139.5 (C), 138.0 (C), 135.4 (C), 132.9 (C), 132.3 (C), 130.1 (C), 129.7 (C), 127.0 (CH), 126.9 (CH), 126.7 (CH), 126.6 (CH), 123.8 (CH), 123.2 (CH), 122.8 (CH), 122.2 (C), 121.3 (C), 119.7 (CH), 119.3 (CH), 69.7 (CH_2), 43.7 (CH), 40.3 (CH_2), 22.1 (CH_3), 19.2 (CH_3), 12.3 ppm (CH_3). MS (Maldi, α-cyano-4-hydroxycinnamic acid) calcd for $C_{58}H_{46}O_2$: 775.0, found: 774.7.

71 Bisbenzo[c]chromene-thioxanthene double motor (BCS)

In a dry nitrogen atmosphere in toluene solution, thioketone **82** (156 mg, 0.30 mmol) was stirred at room temperature. Three equivalents of freshly prepared diazo-compound **84** were added in portions over 5 h; for every portion, a separate oxidation of the precursor hydrazone was performed by stirring with 1 eq Ag_2O and excess $MgSO_4$ and subsequent filtration over celite. Formation of the product was followed by ^{1}H NMR spectroscopy; the first coupling proceeds relatively quickly, but the second coupling requires more time. Three days of room temperature stirring resulted in a mixture of compounds. Filtration of undissolved solids and ^{1}H NMR analysis of the solid gave the *RS*-diastereomer as a double episulfide. This was not further purified but directly refluxed in toluene overnight in the presence of 250 eq PPh_3 (less PPh_3 results in longer reaction times, during which degradation of probably the episulfide mixture occurs). In a separate sequence, the (*RR*/*SS*) racemate was obtained by crystallisation from PhMe of the filtered reaction mixture, after flash column chromatography using chloroform and silica gel to remove part of the side products. The crude episulfide was not purified extensively nor characterised, but refluxed in the presence of 250 eq. PPh_3 in PhMe overnight.

Removal of PPh_3 was achieved by stirring with Merrifield Resin in acetone and subsequent filtration.[40] Washing of the residu with acetone and collection of the filtrate afforded the (*RR*/*SS*)-**71** racemate, which was purified by crystallisation from toluene. Washing of the residu with chloroform afforded (*RS*)-**71**, which was further purified by crystallisation from toluene. Assigment of the diasteromers was performed by HPLC (AD-column, heptane : isopropanol = 98 : 2): the least soluble compound is the wanted meso *RS*-diasteromer, which gives a single peak at r_F = 4.3 min. The (*RR*/*SS*) racemate gives two peaks in the same experiment, at r_F = 4.7 and 5.4 min. and was obtained pure.

RR/*SS*-diastereomer (episulfide) ^{1}H NMR (500 MHz, $CDCl_3$): δ 7.91 (d, *J* = 7.8 Hz, 2H), 7.64 (d, *J* = 7.8 Hz, 2H), 7.42 (d, *J* = 7.6 Hz, 2H), 7.29 – 7.15 (m, 8H), 7.07 (t, *J* = 7.6 Hz, 2H), 6.62 (s, 2H), 4.80 (d, *J* = 12.2 Hz, 2H), 4.71 (d, *J* = 12.2 Hz, 2H), 3.08 (dd, *J* = 15.7, 6.4 Hz, 2H), 2.43 (s, 6H), 2.22 (d, *J* = 14.6 Hz, 2H), 2.03 (s, 6H), 1.03 ppm (d, *J* = 6.9 Hz, 6H). ^{13}C NMR (500 MHz, $CDCl_3$): 153.3, 143.6, 139.0, 136.5, 136.5, 135.7, 132.2, 130.6, 130.1, 129.8, 129.3, 128.8, 127.5, 126.9, 126.8, 126.3, 125.1, 123.3, 122.8, 119.8, 71.4, 69.4, 61.64, 39.9, 36.4, 21.8, 19.6, 11.8 ppm. MS (Maldi, α-cyano-4-hydroxycinnamic acid) calcd for $C_{58}H_{46}O_2S_4$: 902.2, found: 902.5. Alkene (*RR*/*SS*)-**71**: ^{1}H NMR (500 MHz, $CDCl_3$): δ 7.97 (d, *J* = 7.7 Hz, 2H), 7.59 (d, *J* = 7.6 Hz, 2H), 7.55 (d, *J* = 7.6 Hz, 2H), 7.31 (t, *J* = 7.5 Hz, 2H), 7.22 – 7.17 (m, 6H), 7.10 (t, *J* = 7.3 Hz, 2H), 6.94 (s, 2H), 4.91 (d, *J* = 12.2 Hz, 2H), 4.80 (d, *J* = 12.2 Hz, 2H), 4.17 (m, 2H),3.36 (dd, *J* = 15.5, 6.1 Hz, 2H), 2.52 (d, *J* = 15.3 Hz, 2H), 2.21 (s, 6H), 21.40 (s, 6H), 0.72 ppm (d, *J* = 6.7 Hz, 6H). ^{13}C NMR (500

MHz, $CDCl_3$): 154.1 (C), 146.6 (C), 145.8 (C), 141.2 (C), 137.6 (C), 136.1 (C), 135.2 (C), 134.4 (C), 132.3 (C), 130.4 (C), 129.6 (C), 128.3 (CH), 128.3 (CH), 127.6 (CH), 127.4 (CH), 126.4 (CH), 126.3 (CH), 126.0 (CH), 125.9 (CH), 122.9 (C), 122.8 (CH), 120.4 (C), 69.5 (CH_2), 38.4 (CH_2), 36.9 (CH), 21.2 (CH_3), 19.3 (CH_3), 12.3 (CH_3). MS (Maldi, α-cyano-4-hydroxycinnamic acid) calcd for $C_{58}H_{46}O_2S_2$: 838.3, found: 838.3.

RS-diastereomer (episulfide) ^{1}H NMR (500 MHz, $CDCl_3$): δ 7.89 (d, *J* = 7.6 Hz, 2H), 7.64 (d, *J* = 7.5 Hz, 2H), 7.41 (d, *J* = 7.5 Hz, 2H), 7.29 – 7.18 (m, 8H), 7.00 (t, *J* = 7.1 Hz, 2H), 6.83 (s, 2H), 4.78 (d, *J* = 11.9 Hz, 2H), 4.67 (d, *J* = 12.0 Hz, 2H), 3.73 (m, 2H), 3.08 (m, 2H), 2.47 (s, 6H), 2.20 (d, *J* = 15.4 Hz, 2H), 2.08 (s, 6H), 1.03 ppm (d, *J* = 6.9 Hz, 6H). Alkene (*RS*)-**71**: ^{1}H NMR (500 MHz, $CDCl_3$): δ 7.76 (d, *J* = 7.6 Hz, 2H), 7.59 (d, *J* = 7.8 Hz, 2H), 7.56 (d, *J* = 7.8 Hz, 2H), 7.43 (m, 4H), 7.30 (t, *J* = 7.5 Hz, 2H), 7.18 (m, 4H), 7.04 (s, 2H), 4.92 (d, *J* = 12.4 Hz, 2H), 4.77 (d, *J* = 12.2 Hz, 2H), 4.16 (m, 2H), 3.36 (dd, *J* = 15.2, 6.2 Hz, 2H), 2.51 (d, *J* = 8.9 Hz, 2H), 2.19 (s, 6H), 1.46 (s, 6H), 0.72 ppm (d, *J* = 6.7 Hz, 6H). MS (Maldi, α-cyano-4-hydroxycinnamic acid) calcd for $C_{58}H_{46}O_2S_2$: 838.3, found: 838.1.

72 Bisbenzo[c]chromene diketone

The eliminated product **81** (159 mg, 0.33 mmol) was added to a stirred mixture of concentrated H_2SO_4 in a nitrogen atmosphere at room temperature. After 2 h, the mixture was poured on ice, extracted with $CHCl_3$, washed, dried and the solvent evaporated to result in 159 mg (100%) of diketone **72** as a white solid. ^{1}H NMR (400 MHz, $CDCl_3$): δ 7.52 (s, 2H), 5.03 (s, 4H), 3.25 (dd, *J* = 17.2, 8.1 Hz, 2H), 2.94 (s, 6H), 2.68 (m, 2H), 2.56 (d, *J* = 17.2 Hz, 2H), 2.21 (s, 6H), 1.31 ppm (d, *J* = 7.3 Hz, 6H). ^{13}C NMR (500 MHz, $CDCl_3$): 209.7 (CO), 159.0 (C), 154.7 (C), 134.2 (C), 133.1 (C), 129.1 (C), 128.2 (C), 123.6 (CH), 122.7 (C), 120.6 (C), 69.5 (CH_2), 42.4 (CH), 33.3 (CH_2), 17.4 (CH_3), 16.9 (CH_3), 11.1 ppm (CH_3). MS (EI, %): m/z = 478 (100), 463 (17), 437 (10). HRMS calcd for $C_{32}H_{30}O_4$: 478.2144, found: 478.2118.

73 Bis(benzo[c]chromene)[37]

A schlenk vessel with a dry nitrogen atmosphere was charged with 1.16 g (2.3 mmol) **23**, 15% $Pd(OAc)_2$, 22.5% $P(cy)_3$ and 3 eq. oven-dried K_2CO_3 in 35 ml DMA that was dried on CaH_2 and distilled under vacuum. The starting material did not dissolve, but after 15 h heating at 130°C a clear solution was obtained, which was filtered over silica gel and the solvent removed, and DMA was removed by kugelrohr distillation. This resulted in 714 mg (100%) of **24** as a yellow-brown solid. ^{1}H NMR (400 MHz, $CDCl_3$): δ 7.57 (s, 2H), 7.00 (d, *J* = 7.7 Hz, 2H), 6.84 (d, *J* = 7.7 Hz, 2H), 4.98 (s, 4H), 2.66 (s, 6H), 2.28 (s, 6H). ^{13}C NMR (400 MHz, $CDCl_3$): δ 154.4 (C), 133.3 (C), 132.6 (C), 129.9 (CH), 129.5 (C), 124.7 (CH), 124.0 (C), 122.7 (CH), 122.6 (C), 69.2 (CH_2), 22.5 (CH_3), 15.9 (CH_3). MS (EI, %): m/z = 342 (100), 171 (9). HRMS calcd for $C_{24}H_{22}O_2$: 342.1620, found: 342.1603.

74 2,2'-(2,5-Dibromo-1,4-phenylene)bis(methylene)bis(oxy)bis(1,4-dimethylbenzene)

An acetone-solution of 2.97 g of **76** (7.03 mmol) was brought to reflux in the presence of an excess of K_2CO_3, 1% NaI and 2.1 eq. of 2,5-dimethylphenol. After 15 h the mixture was

diluted with 8 volume-eq. of H_2O and filtered. Washing with $NaHCO_3$-solution and H_2O resulted in a white solid, with was dried on air to result in pure **74** (3.37 g, 6.73 mmol, 96%). ^{1}H NMR (400 MHz, $CDCl_3$): δ 7.81 (s, 2H), 7.05 (d, *J* = 7.3 Hz, 2H), 6.72 (d, *J* = 7.3 Hz, 2H), 6.69 (s, 2H), 5.05 (s, 4H), 2.32 (s, 6H), 2.28 (s, 6H). ^{13}C NMR (400 MHz, $CDCl_3$): δ 156.13 (C), 137.82 (C), 136.7 (C), 132.1 (CH), 130.6 (CH), 123.8 (C), 121.7 (CH), 120.9 (C), 112.4 (CH), 68.6 (CH_2), 21.4 (CH_3), 16.0 (CH_3). MS (EI, %): m/z = 504 (55), 383 (100), 304 (23), 262 (47), 223 (20). HRMS calcd for $C_{24}H_{24}Br_2O_2$: 502.0143, found: 502.0123.

80 Friedel-Crafts acylation product

Bisbenzo[c]chromene **73** was inserted in a 50 ml 2-necked flask under a dry nitrogen environment, and 2.25 eq. of $AlCl_3$ and α-chloro-β-methylpropionic acid chloride[38] was added. The mixture was stirred as a DCM solution at room temperature overnight. The mixture was quenched on ice, extracted with DCM, washed, dried over $MgSO_4$ and the solvent evaporated to result in pure **80** as a yellow solid consisting of 2 diastereomers (one regioisomer, 82%).^{1}H NMR (400 MHz, $CDCl_3$): δ 7.50 (s, 2H), 7.36 (s, 2H), 4.99 (m, 2H), 3.92 (m, 2H), 3.70 (m, 2H), 3.60 (m, 2H), 2.68 (s, 6H), 2.28 (S, 6H), 1.27 ppm (m, 6H). ^{13}C NMR (500 MHz, $CDCl_3$): δ 204.6 (CO), 156.8 (C), 133.8 (C), 133.2 (C), 132.9 (C), 130.4 (CH), 129.2 (C), 124.5 (C), 123.9 (CH), 123.7 (C), 69.3 (CH_2), 46.6 (CH), 46.3 (CH_2), 20.4 (CH_3), 15.9 (CH_3), 15.8 ppm (CH_3). MS (EI, %): m/z = 550 (40), 514 (36), 473 (100), 437 (43). HRMS calcd for $C_{32}H_{32}O_4Cl_2$: 550.1678, found: 550.1656.

81 Elimination product

Compound **80** (131 mg, 0.237 mmol) was dissolved in $CHCl_3$/NEt_3 (1/1 V/V) and refluxed for several days while monitoring the reaction by TLC. The solvent was evaporated and the crude product purified by column chromatography to result in the pure product (99 mg, 87%). ^{1}H NMR (400 MHz, $CDCl_3$): δ 7.57 (s, 2H), 7.00 (d, *J* = 7.7 Hz, 2H), 6.84 (d, *J* = 7.7 Hz, 2H), 4.98 (s, 4H), 2.66 (s, 6H), 2.28 (s, 6H). ^{13}C NMR (400 MHz, $CDCl_3$): δ 154.4 (C), 133.3 (C), 132.6 (C), 129.9 (CH), 129.5 (C), 124.7 (CH), 124.0 (C), 122.7 (CH), 122.6 (C), 69.2 (CH_2), 22.5 (CH_3), 15.9 (CH_3). MS (EI, %): m/z = 342 (100), 171 (9). HRMS calcd for $C_{24}H_{22}O_2$: 342.1620, found: 342.1603.

82 Bisbenzo[c]chromene dithioketone

In toluene solution, **82** (49 mg, 102 µmol) was refluxed with 2.1 eq. Lawesons reagent for 2 h. The reaction mixture was cooled to room temperature and quickly flushed over toluene-presaturated neutral aluminium oxid with the aid of vacuum, and then rinsed with toluene until the filtrate was without colour. Because the product degrades on silica gel fast, and degrades on aluminium oxide as well, but slower, the speed with which this is performed determines the yield. After evaporation of solvents the product is obtained pure as a red mixture of diastereomers (45 mg, 88%). ^{1}H NMR (400 MHz, $CDCl_3$): δ 7.49 (2*s, 2H), 5.04 (s, 4H), 3.34 (dd, *J* = 17.6, 7.3 Hz, 2H), 3.10 (s, 6H), 3.04 (m, 2H), 2.72 (d, *J* = 18.0 Hz, 2H), 2.25 (s, 6H), 1.44 ppm (2*d, 6H). ^{13}C NMR (400 MHz, $CDCl_3$): 249.3 (CS), 158.8 (C), 156.3 (C), 138.8 (C), 136.3 (C), 133.0 (C), 129.2 (C), 124.2 (CH), 123.8 (C), 120.3

(C), 69.6 (CH_2), 55.4 (CH), 38.0 (CH_2), 22.2 (CH_3), 21.1 (CH_3), 11.7 ppm (CH_3). MS (EI, %): m/z = 510 (100), 494 (28), 478 (60). HRMS calcd for $C_{32}H_{30}O_2S_2$: 510.1687, found: 510.1673.

[1] (a) Browne, W. R.; Feringa, B. L., *Nat. Nanotechnol.* **2006**, *1*, 25. (b) Leigh, D. A.; Zerbetto, F.; Kay, E. R., *Angew. Chem. Int. Ed.* **2007**, *46*, 72. (c) Astumian, R. D., *Phys. Chem. Chem. Phys.* **2007**, *9*, 5067. (d) Paxton, W. F.; Kisler, K. C.; Olmeda, C. O.; Sen, A.; St.Angelo, S. K.; Cao, Y.; Mallouk, T. E.; Lammert, P. E.; Crespi, V. H., *J. Am. Chem. Soc.* **2004**, *126*, 13424. (e) Catchmark, J. M.; Subramanian, S.; Sen, A., *Small* **2005**, *1*, 202. (f) Kline, T. R.; Paxton, W. F.; Mallouk, T. E.; Sen, A., *Angew. Chem. Int. Ed.* **2005**, *44*, 744. (g) Fournier-Bidoz, S.; Arsenault, A. C.; Manners, I.; Ozin, G. A., *Chem. Commun.* **2005**, 441.

[2] a) Zhu, Y.; Fujiwara, M., *Angew. Chem. Int. Ed.* **2007**, *46*, 2241. b) Ismagilov, R. F.; Schwartz, A.; Bowden, N.; Whitesides, G. M., *Angew. Chem. Int. Ed.* **2002**, *41*, 652. c) Vicario, J.; Eelkema, R.; Browne, W. R.; Meetsma, A.; La Crois, R. M.; Feringa, B. L., *Chem. Commun.* **2005**, 3936.

[3] *Molecular Motors*; Schliwa, M., Ed.; Wiley-VCH: Weinheim, Germany, **2003**.

[4] Shirai, Y.; Osgood, A. J.; Zhao, Y.; Kelly, K. F.; Tour, J. M., *Nano Lett.* **2005**, *5* (11), 2330. (b) Grill, L.; Rieder, K. –H.; Moresco, F.; Rapenne, G.; Stojkovic, S.; Bouju, X.; Joachim, C., *Nat. Nanotechnol.* **2007**, *2*, 95.

[5] (a) Haidekker, M. A.; Theodorakis, E. A., *Org. Biomol. Chem.* **2007**, *5*(11), 1669. (b) Haidekker, M. A.; Brady, T. P.; Lichlyter, D.; Theodorakis, E. A., *Bioorg. Chem.* **2005**, *33*(6), 415. (c) Hurenkamp, J. H., *Tuning Energy Transfer between Chromophores*, PhD thesis, **2008**. (d) Turro, N. J., *Modern Molecular Photochemistry* , University Science Books, Sausalito, California (**1991**). (e) HMontalti, M.; Credi, A.; Prodi, L.; Gandolfi, M. T., *Handbook of photochemistry,* 3rd ed., CRC (**2006**).

[6] Pollard, M. M.; Meetsma, A.; Feringa, B. L., *Org. Biomol. Chem.* **2008**, *6*, 507.

[7] Bymaster, D. L.; Pickering, R. E.; Dobbs, T. K.; Eisenbraun, E. J., *Journal of Labeled Compounds and Radiopharmaceuticals* **1986**, *23* (6), 657.

[8] (a) Royals, E. E.; Greene, J. L, *J. Org. Chem* **1958**, *23*, 1437. (b) Shyadehi, A. Z.; Harding, J. J., *J. Labelled Compound Radiopharm* **1999**, *42*, 207.

[9] (a) Pijper, T. C.; Pijper, D.; Pollard, M. M.; Dumur, F.; Davey, S. D.; Meetsma, A.; Feringa, B. L., *manuscript in preparation.* (b) Furrow, M. E.; Myers, A. G., *J. Am. Chem. Soc.* **2004**, *126*, 5436. (c) Furrow, M. E.; Myers, A. G., *J. Am. Chem. Soc.* **2004**, *126*, 12222.

[10] (a) Ter Wiel, M. K. J., *Basic Molecular Devices*, Ph. D. Thesis, **2004**, University of Groningen. (b) Wesenhagen, P, *Substituent Effects on Molecular Motors*, Graduate report, **2005**, University of Groningen.

[11] Hays, S. M.,; Aylward, L. L., *Regul. Toxicol. Pharmacol.* **2003**, *37*, 202.

[12] (a) Palmer, B. D.; Rewcastle, G. W.; Atwell, G. J.; Baguley, B. C.; Denny, W. A, *J. Med. Chem.* **1988**, *31*, 707. (b) Ruiz, N.; Boun, C.; Pukol, M. D.; Guillaumet, G.; Coudert, G. *Synth. Commun.* **1996**, *26*, 2057. (c) Lee, H. H.; Palmer, B. D.; Boyd, M; Baguley, B. C.; Denny, W. A., *J. Med. Chem.* **1992**, *35*, 258.

[13] Lee, H. H.; Denny, W. A., *J. Chem. Soc., Perkin Trans. 1,* **1990**, 1071.

[14] (a) Tomita, M., *J. Pharm. Soc. Jpn.* **1932**, *52*, 49. (b) Gilman, H.; Dietrich, J. J. *J. Am. Chem. Soc.* **1957**, *79*, 1439.

[15] (a) Pachaly, P.; Schäfer, M., *Arch. Pharm.* **1989**, *322*, 477. (b) Blair, E. H. (ed), Advances in Chemistry, no 120., A. C. S., Washington, D. C. (**1973**).

[16] Ramsden, C. A., J. Chem. Soc., Perkin Trans. 1, **1981**, 2456.

[17] (a) Gray, A. P.; Cepa, S. P.; Cantrell, J. S., *Tetrahedron Lett*. **1975**, 2873. (b) Kende, A. S.; DeCamp, M. R., *Tetrahedron Lett.* **1975**, 2877.

[18] Anjaneyulu, B.; Govindachari, T. R.; Viswanathan, N., *Tetrahedron* **1971**, *27*, 439.

[19] (a) Pohland, A. E.; Yang, G. C., *J. Agr. Food Chem.* **1972**, *20*, 1093. (b) Gray, A. P.; Cepa, S. P.; Solomon, I. J.; Aniline, O. *J. Org. Chem.* 1976, *41*, 2435.

[20] Kende, A. S.; Wade, J. J.; Ridge, D.; Poland, A., *J. Org. Chem.* **1974,** *39*, 931.

[21] Eastmond, G. C.; Paprotny, J.; Steiner, A.; Swanson, L, *New. J. Chem.* **2001**, *25*, 379.

[22] Hellberg, J.; Pelcman, M. E., *Tetrahedron Lett.* **1994**, *35*, 1769.

[23] Hellberg, J.; Dahlstedt, E.; Pelcman, M. E., *Tetrahedron* **2004**, *60*, 8899.

[24] Litvak, V. V.; Goryunov, L. I.; Shteingarts, V. D., *J. Org. Chem. USSR* **1981**, *22*, 138 (*Engl. Trans*.).

[25] Sutherland, R. G.; Piorko, A.; Lee, C. C.; Simonsen, S. H.; Lynch, V. M., *J. Heterocycl. Chem.* **1988**, *25*, 1911.

[26] Sawyer, J. S., *Tetrahedron* **2000**, *56*, 5045. (b)

[27] Thomas, A. W.; Ley, S. V., *Angew. Chem. Int. Ed.* **2003**, *42*, 5400.

[28] Prim, D.; Campagne, J. M.; Joseph, D.; Andrioletti, B., *Tetrahedron* **2002**, *58*, 2041.

[29] Jung, K-Y; Koreeda, M., *J. Org. Chem.* **1989**, *54*, 5667.

[30] a) Burgos, C. H.; Barder, T. E.; Huang, X.; Buchwald, S. L., *Angew. Chem. Int. Ed.* **2006**, *45*, 4321. b) Aranyos, A.; Old, D. W.; Kiyomori, A.; Wolfe, J. P.; Sadighi, J. P.; Buchwald, S. L., *J. Am. Chem. Soc.* **1999**, *121*, 4369.

[31] a) Zhang, S.; Zhang, D.; Liebeskind, L. S., *J. Org. Chem.* **1997**, *62*, 2312. b) Marcoux, J.-F.; Doye, S.; Buchwald, S. L., *J. Am. Chem. Soc.* **1997**, *119*, 10539. c) Gujadhur, R.; Venkataraman, D., *Synth. Commun.* **2001**, *31*, 2865. d) Ouali, A.; Spindler, J.-F.; Cristau, H.-J.; Taillefer, M. *Adv. Synth. Catal.* **2006**, *348*, 499.

[32] Nicolaou, K. C.; Boddy, C. N. C.; Natarajan, S.; Yue, T. Y.; Li, H.; Bräse, S.; Ramanjulu, J. M., *J. Am. Chem. Soc.* **1997**, *119*, 3421. b) Nicoloau, K. C.; Natarajan, S.; Li, H.; Jain, N. F.; Hughes, R.; Solomon, M. E.; Ramanjulu, J. M.; Body, C. N. C.; Takayanagi, M., *Angew. Chem. Int. Ed.* **1998**, *37*, 2708.

[33] Olah, G. A.; Arvanaghi, M; Vankar, Y. D., *J. Org. Chem* **1980**, 45, 3531.

[34] a) Rayne, S.; Sasaki, R.; Wan, P., *Photochem. Photobiol. Sci.* **2005**, *4*, 876. b) Guan, B.; Wan, P., *J. Photochem. Photobiol.A: Chem.* **1994**, *80*, 199.

[35] a) Huang, C.-G.; Shukla, D.; Wan, P., *J. Org. Chem.* **1991**, *56*, 5437. b) Huang, C.-G.; Beveridge, K. A; Wan, P., *J. Am. Chem. Soc.* **1991**, *113*, 7676.

[36] Bonifacio, M. C.; Robertson, C. R.; Jung, J.-Y.; King, B. T., *J. Org. Chem.* **2005**, *70*, 8522.

[37] Campeau, L.-C.; Parisien, M.; Jean, A.; Fagnou, K., *J. Am. Chem. Soc.* **2006**, *128*, 581.

[38] Kharasch, M. S.; Brown, H. C., *J. Am. Chem. Soc.* **1940**, *62*, 925.

[39] Katz, T. J.; Sudhakar, A.; Teasley, M. F.; Gilbert, A. M.; Geiger, W. E.; Robben, M. P.; Wuensch, M.; Wards, M. D., *J. Am. Chem. Soc.* **1993,** *115*, 3182.

[40] Lipshutz, B. H.; Blomgren, P. A., *Org. Lett.* **2001**, *3* (12), 1869.

[41] Gaussian 03, Revision C.02,M. J. Frisch, G. W. Trucks, H. B. Schlegel, G. E. Scuseria, M. A. Robb, J. R. Cheeseman, J. A. Montgomery, Jr., T. Vreven, K. N. Kudin, J. C. Burant, J. M. Millam, S. S. Iyengar, J. Tomasi, V. Barone, B. Mennucci, M. Cossi, G. Scalmani, N. Rega, G. A. Petersson, H. Nakatsuji, M. Hada, M. Ehara, K. Toyota, R. Fukuda, J. Hasegawa, M. Ishida, T. Nakajima, Y. Honda, O. Kitao, H. Nakai, M. Klene, X. Li, J. E. Knox, H. P. Hratchian, J. B. Cross, C. Adamo, J. Jaramillo, R. Gomperts, R. E. Stratmann, O. Yazyev, A. J. Austin, R. Cammi, C. Pomelli, J. W. Ochterski, P. Y. Ayala, K. Morokuma, G. A. Voth, P. Salvador, J. J. Dannenberg, V. G. Zakrzewski, S. Dapprich, A. D. Daniels, M. C. Strain, O. Farkas, D. K. Malick, A. D. Rabuck, K. Raghavachari, J. B. Foresman, J. V. Ortiz, Q. Cui, A. G. Baboul, S. Clifford, J. Cioslowski, B. B. Stefanov, G. Liu, A. Liashenko, P. Piskorz, I. Komaromi, R. L. Martin, D. J. Fox, T. Keith, M. A. Al-Laham, C. Y. Peng, A. Nanayakkara, M. Challacombe, P. M. W. Gill, B. Johnson, W. Chen, M. W. Wong, C. Gonzalez, and J. A. Pople, Gaussian, Inc., Wallingford CT, 2004.

[42] A guide to recording fluorescence quantum yields, Jobin Yvon Ltd. Accessed via http://www.jobinyvon.com/SiteResources/Data/MediaArchive/files/Fluorescence/applications/quantumyieldstrad.pdf

[43] A more elaborate discussion of the techniques involved will be presented later; here the focus in on the results.

[44] Scheibye, S.; Shabana, R.; Lawesson, S. O.; Roemming, C., *Tetrahedron* **1982**, *38* (7), 993.

[45] Due to the insolubility, integral values could not be determined accurately.

[46] Futamura, S.; Zong, Z.-M., *Bull. Chem. Soc. Jpn*. 1992, 65, 345.